Cancer Biol Med 2026. doi: 10.20892/j.issn.2095-3941.2025.0236

ORIGINAL ARTICLE

HBx-mediated GPT2 suppression promotes liver cancer development by downregulating ADH1A

Hongjuan You[1]*, Xing Wang[1,2]*, Ruyu Liu[3], Yuxin Wang[1], Huanyang Zhang[1], Lihong Ma[1], Ensi Bao[1], Yujie Zhong[1], Xiangye Liu[1], Delong Kong[1], Xiucheng Pan[4], Xiaocui Li[1], Suping Qin[1], Kuiyang Zheng[1,5], Chen Li[1], Renxian Tang[1,5], Fanyun Kong[1]

[1]Jiangsu Key Laboratory of Immunity and Metabolism, Department of Pathogenic Biology and Immunology, School of Basic Medical Sciences, Xuzhou Medical University, Xuzhou 221004, China; [2]Department of Clinical Laboratory, Heping Hospital Affiliated to Changzhi Medical College, Changzhi 046000, China; [3]Department of Hepatology Division, Beijing Ditan Hospital Affiliated to Capital Medical University Xuzhou Hospital and Xuzhou Seventh People's Hospital, Xuzhou 221004, China; [4]Department of Infectious Diseases, The Affiliated Hospital of Xuzhou Medical University, Xuzhou 221006, China; [5]National Demonstration Center for Experimental Basic Medical Sciences Education, Xuzhou Medical University, Xuzhou 221004, China

ABSTRACT

Objective: Hepatitis B virus (HBV) is the primary driver of liver cancer (LC), a malignancy characterized by extensive metabolic reprogramming. However, the specific mechanisms linking viral oncoproteins to metabolic dysregulation in LC remain incompletely understood. This study was aimed at investigating the function of the metabolic enzyme GPT2 in hepatocarcinogenesis, focusing on its regulation by HBV X protein (HBx) and its effects on downstream signaling pathways.

Methods: We combined analysis of multiple patient cohorts with *in vitro* and *in vivo* functional assays to determine the clinical relevance and function of GPT2. Co-immunoprecipitation, ubiquitination assays, and targeted pharmacological or genetic manipulations were used to delineate the signaling cascade.

Results: GPT2 was significantly downregulated in LC, and its low expression correlated with poor patient survival. Functionally, GPT2 loss promoted LC cell proliferation, migration, and lipid accumulation. Mechanistically, GPT2 was found to suppress the mTOR pathway by disrupting the AKT–mTOR interaction and leading to upregulation of ADH1A. In turn, ADH1A facilitates CBL-mediated ubiquitination and degradation of LSD1, a key driver of lipogenesis. Critically, the HBV oncoprotein HBx functions as a molecular adaptor that recruits TRIM25 to GPT2, thus leading to GPT2 ubiquitination and proteasomal degradation. Moreover, HBx-mediated loss of GPT2 was found to drive tumor progression by modulating the mTOR–ADH1A–LSD1 axis and enhancing lipid synthesis.

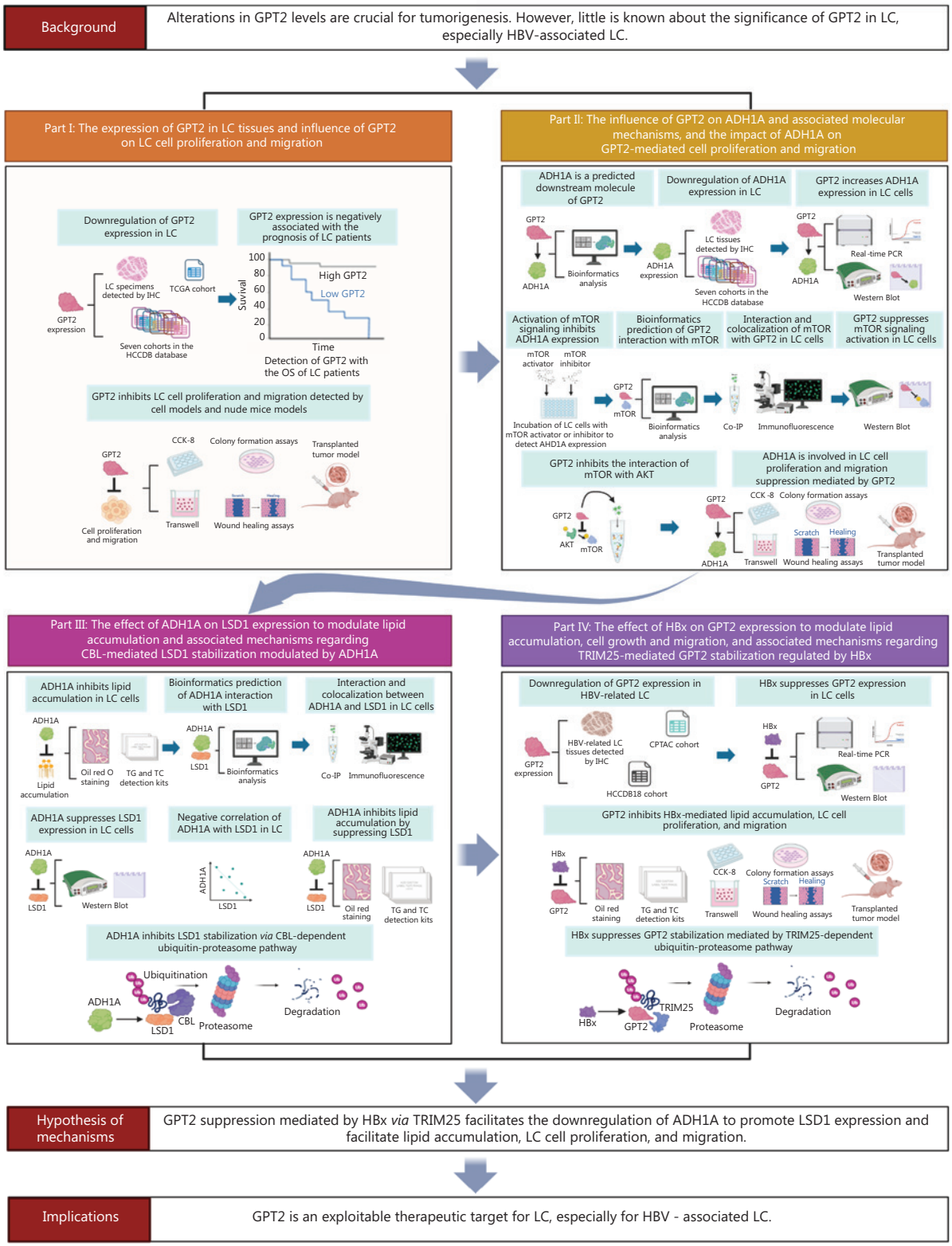
Conclusions: Our study delineated a novel HBx–TRIM25–GPT2–ADH1A–LSD1 signaling axis promoting virus-associated hepatocarcinogenesis. GPT2 was identified as a critical metabolic tumor suppressor hijacked by HBV and a promising therapeutic target for treating HBV-associated LC.

KEYWORDS Liver cancer; HBx; GPT2; ADH1A; CBL; LSD1

Introduction

Liver cancer (LC), including hepatocellular carcinoma, cholangiocarcinoma, and hepatoblastoma[1], is a global health concern. The high mortality rate associated with hepatic tumors underscores a need to clarify the molecular mechanisms promoting LC progression, which might reveal novel therapeutic opportunities. Metabolic reprogramming, a defining feature of cancer, benefits malignant cells by allowing them to adapt to increased energy demands, and subsequently undergo rapid proliferation and metastasis[2,3]. Dysregulated lipid metabolism has been strongly implicated in LC pathogenesis[4]. Therefore, identifying key regulators of lipid metabolism in LC might provide promising targets for therapeutic interventions.

*These authors contributed equally to this work.
Correspondence to: Chen Li, Renxian Tang, and Fanyun Kong
E-mail: lichen20377@163.com, tangrenxian-t@163.com, and kong.fanyun@163.com
ORCID ID: https://orcid.org/0000-0002-9293-0808, https://orcid.org/0000-0002-4205-1071, and https://orcid.org/0000-0002-4551-5687
Received May 18, 2025; accepted February 25, 2026;
published online May 19, 2026.
Available at www.cancerbiomed.org
©2026 The Authors. Creative Commons Attribution-NonCommercial 4.0 International License (CC BY-NC 4.0)



Study flowchart GPT2 suppression mediated by HBx facilitates downregulation of ADH1A and promotion of LSD1 expression, thus leading to lipid accumulation, LC cell proliferation, and migration. Part I describes detection of GPT2 expression in LC tissues and the influence of GPT2 on LC cell proliferation and migration. Part II outlines the influence of GPT2 on ADH1A expression and associated mechanisms, and the effects of ADH1A on GPT2-mediated cell proliferation and migration. Part III examines ADH1A's effects on LSD1 expression, and its modulation of lipid accumulation

and related mechanisms underlying CBL-mediated LSD1 stabilization. Part IV describes the effects of GPT2 on HBx-modulated lipid accumulation, cell growth and migration, and associated mechanisms underlying TRIM25-mediated GPT2 stabilization regulated by HBx. This study highlights GPT2, its downstream molecules, and regulators in hepatocarcinogenesis. GPT2 is an exploitable therapeutic target for LC, particularly for HBV-associated LC. IHC, immunohistochemistry; LC, liver cancers; KM, Kaplan–Meier; OS, overall survival; TC, total cholesterol; TG, triglycerides.

Glutamic-pyruvic transaminase 2 (GPT2) is an important enzyme that participates in glutamine metabolism, and plays crucial regulatory roles in glycometabolism and autophagy across diverse cell types[5-7]. GPT2 has been implicated in the progression of cancers including glioblastoma, bladder cancer, and breast cancer[5,7,8]. However, its expression patterns, clinical and biological importance, and regulatory mechanisms in LC remain largely unknown.

Alcohol dehydrogenase 1A (ADH1A), an enzyme that oxidizes ethanol[9], promotes malignant progression in several cancers, including lung and gastric carcinomas[10,11]. In LC, ADH1A expression is downregulated[12,13], and mTOR signaling contributes to this downregulation *via* histone deacetylase 1 (HDAC1)-mediated transcriptional inhibition[14]. However, the biological processes and mechanisms underlying ADH1A expression in LC require further investigation.

Lysine-specific demethylase 1 (LSD1), a well-known histone demethylase, is frequently overexpressed in breast, gastric, and pancreatic cancers, and is known to contribute to tumor progression[15-19]. Elevated LSD1 expression has also been observed in LC[20,21] and is significantly associated with poor prognosis[22]. However, the factors regulating LSD1 expression in LC remain unclear.

Most LC cases in Asia and Africa are associated with hepatitis B virus (HBV) infection[23,24]. The HBV-encoded X protein (HBx) has a key role in LC pathogenesis[25,26]. For example, HBx modulates the stability of proteins such as LASP1 and GRP78 by interfering with their interaction with ubiquitin ligases such as SYVN1 and TRIM25, thereby influencing regulators such as GLUD1 and MAN1B1, and affecting LC cell biology[27,28]. However, whether HBx might regulate GPT2, ADH1A, and LSD1, and consequently promote hepatocarcinogenesis, remains unclear.

Herein, we investigated the role of GPT2 in LC. GPT2 was found to be downregulated in LC, and its low expression promoted ADH1A silencing, thus increasing LSD1 levels and lipid accumulation. Furthermore, HBx was found to decrease GPT2 stability by strengthening the interaction between GPT2 and TRIM25, downregulating ADH1A, upregulating LSD1, and stimulating lipid accumulation. These findings therefore revealed previously unrecognized roles and regulatory mechanisms of GPT2 in hepatocarcinogenesis.

Materials and methods

Reagents and cell culture

Antibodies to Flag tag, GAPDH, HA tag, and AKT; MG132; HBV plasmid; cycloheximide (CHX); TRIM25 expression plasmids; TRIM25 short hairpin RNA (shRNA) plasmids; vectors containing various HBV genes; and other reagents were obtained as previously described[27-30]. Antibodies targeting TRIM25, p-mTOR, FASN, SCD1, Ki67, β-tubulin, LSD1, CBL, GPT2, and mTOR were purchased from ABclonal (Wuhan, China), Zenbio (Chengdu, China), Huabio (Hangzhou, China), and Proteintech (Wuhan, China). The AKT activator SC79, the mTOR pathway activator MHY1485, and its inhibitor AZD8055 were obtained from MedChemExpress (Shanghai, China). Anti-ADH1A was purchased from Santa Cruz Biotechnology (Santa Cruz, CA, USA). Ke Lei Biological Technology (Shanghai, China) provided vectors containing shRNA sequences against GPT2 (5′-GCCCAGAAGATGCTAAGAAACTCGAGTTTCTTAGCATCTTCTGGGCTTT TTT-3′), CBL (5′-GCCGATGTGAAATTAAAGGTATTCAA GAGATACCTTTAATTTCACATCGGCTTTTTT-3′), ADH1A (5′-GGATGCATTAATAACCCATGTTTCAAGAGAACATGGGTTATTAATGCATCCTTTTTT-3′), and LSD1 (5′-GCTACATCTTACCTTAGTCATTT CAAGAGAATGACTAAGGTAAGATGTAGCTTTTTT-3′); Flag-labeled-GPT2 expression plasmid, Flag-labeled-ADH1A expression plasmids, Flag-labeled-CBL expression plasmids, HA-labeled-NEDD4 expression plasmids, and Flag-GPT2 mutant plasmids, including mutants with or without aminotransferase class I and II domains (detailed information can be found in the Pfam database at http://pfam.xfam.org/); GPT2 plasmids (GPT2-Mut) containing C259R, N271T, and V478R mutants[31]; and mTOR mutant plasmids, including C-terminal (with mTOR domain), double-terminal (with FAT domain), and N-terminal deletions of mTOR mutants (with the PI3/4 kinase catalytic domain) (detailed information can be found in the Pfam database). HepG2, HEK293T, and Huh7 cells were cultured, transfected with target plasmids, and selected as previously described[28,29].

Detection of lipids, triglycerides, and cholesterol

The lipid droplet content in the target cells was measured with Oil Red O staining, according to the manufacturer's instructions (Beyotime, Shanghai, China). The concentrations of total cholesterol (TC) and triglyceride (TG) in LC cells were determined with total TC and TG detection kits purchased from Solarbio (Beijing, China).

Clinical samples, immunohistochemistry, and H&E staining

A total of 112 HBV-positive tumor tissues, 88 HBV-negative LC tissues, and 80 adjacent tissues were collected from

Outdo Biotech Co., Ltd. (Shanghai, China), and the Affiliated Hospital of Xuzhou Medical University. The tissues came from patients with LC who were treated with surgical resection. Immunohistochemistry (IHC) analysis was performed to assess the relative expression of GPT2 and ADH1A. Briefly, after deparaffinization, rehydration, and incubation with sodium citrate, the tissues were treated with H_2O_2; blocked with 5% goat serum; incubated with primary antibodies to GPT2 (1:200) and ADH1A (1:400) and subsequently with horseradish peroxidase-conjugated secondary antibodies (1:500); and stained with 3,3′-diaminobenzidine. The tissues were counterstained with hematoxylin. Hematoxylin-eosin (H&E) staining was performed as previously described[32]. GPT2 and ADH1A protein expression levels were calculated as previously described[33,34]. This study was conducted in accordance with the principles of the Declaration of Helsinki and was approved by the Ethics Committee of the Affiliated Hospital of Xuzhou Medical University (approval No. XYFY2022-KL085-01).

Animal transplantation

Four-week-old BALB/c nude mice were obtained from Cavenslasales Company (Changzhou, China). The mice were randomly divided into groups (mice per group $n = 5$) and housed under specific-pathogen-free, temperature-controlled conditions. Matrigel solution (BD Biosciences, New Jersey, USA) (0.1 mL) combined with cell suspensions (0.1 mL, 2×10^7/mL) resuspended in phosphate-buffered saline was injected into the shoulders of nude mice. After rearing for 2–3 weeks, the mice were euthanized, and tumor samples were collected. Tumor weights and volumes were measured as previously described[33]. All animal experiments were approved by the Animal Care and Use Committee of Xuzhou Medical University (approval No. L20210226151).

Bioinformatics analysis

Biological processes associated with GPT2 and ADH1A were predicted with gene set enrichment analysis (GSEA) and the ARCHS[4] database, as previously described[28]. Biological processes associated with LSD1 were predicted with the ARCHS[4] database[35]. Information on GPT2 expression was extracted from The Cancer Genome Atlas (TCGA) and the HCCDB database[36]. LC tissues were divided into low or high GPT2 and ADH1A expression groups for GSEA or univariate survival analysis according to median gene expression levels. GPT2 protein expression data in HBV-associated LC tissues were obtained from the Clinical Proteomic Tumor Analysis Consortium (CPTAC) database[37]. The interaction between GPT2 and mTOR was predicted with the ARCHS[4] database. Information on potential interactions between ADH1A and LSD1 was collected from the PrePPI database[38]. Additionally, the predicted E3 ligases ADH1A and GPT2 were extracted from the UbiBrowser online database[39].

Immunofluorescence analysis

The localization of GPT2, mTOR, LSD1, ADH1A, CBL, and TRIM25 was detected with immunofluorescence. Briefly, after fixation with ice-cold acetone, LC cells were blocked with 5% bovine serum albumin in phosphate-buffered saline. The cells were then treated with primary antibodies targeting GPT2 (1:200), mTOR (1:100), LSD1 (1:100), ADH1A (1:50), CBL (1:300), or TRIM25 (1:200). After being washed 3 times, the cells were incubated with Alexa Fluor 594 (1:300)- or Alexa Fluor 488 (1:300)-conjugated secondary antibodies. The cells were then incubated with DAPI. The results of the immunofluorescence assays were obtained with an Olympus microscope.

Cell proliferation and migration assays

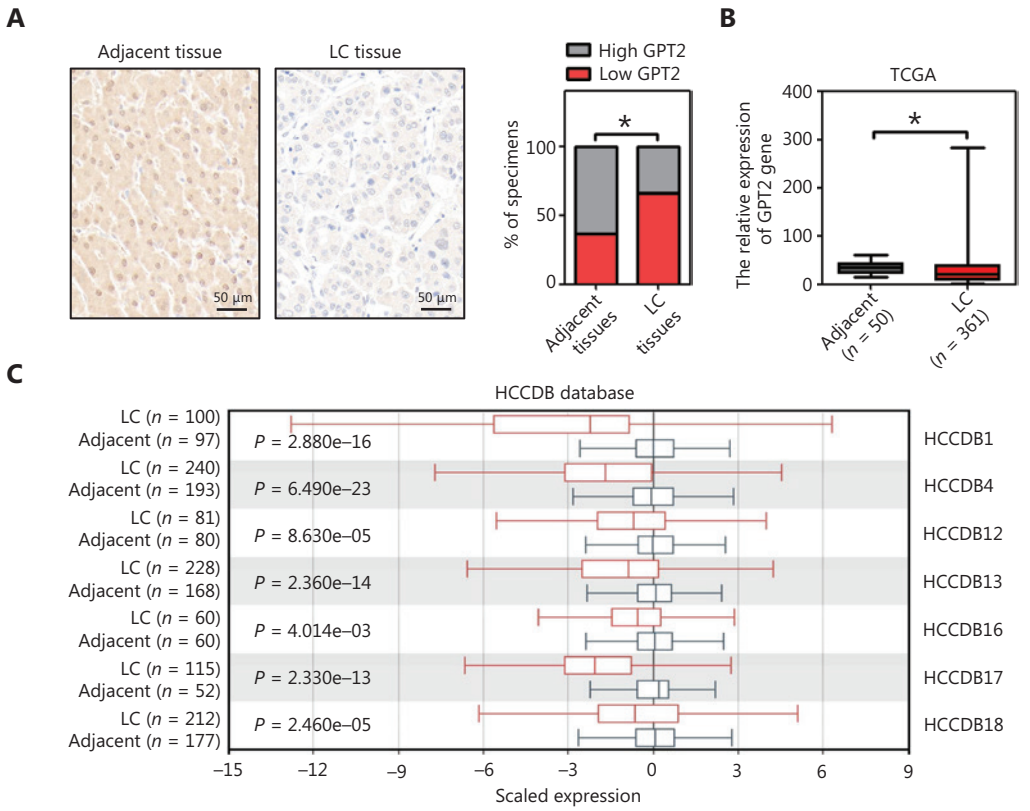
Cell growth efficiency was assessed with Cell Counting Kit-8 (CCK-8) assays, and cell clone formation assays were performed as previously described[34]. To examine cell migration, we conducted a wound-healing experiment combined with a Transwell assay, as previously reported[33].

Real-time polymerase chain reaction (PCR)

The primers for the detection of GPT2 were (F) 5′-GGTCCTACA GTGCTAGCCAGGG-3′ and (R) 5′-AGAA ATGCCGTCACTAGCTCCC-3′, whereas those for the detection of ADH1A were (F) 5′-GTG GCTGTAGG AATCTGTGGC-3′ and (R) 5′-ACTGAGGAATAGCGAG TGGGA-3′. Real-time PCR analysis was performed with SuperReal PreMix Plus reagent (SYBR Green) (Tiangen Biotech, Beijing, China). On the basis of the manufacturer's instructions, the optimized real-time PCR conditions were as follows: 5 min at 95°C, and 35 cycles of 10 s at 95°C, 30 s at 58°C, and 30 s at 72°C. GPT2 and ADH1A levels were normalized to GAPDH levels. The primers were as previously described[40].

Co-immunoprecipitation, Western blot, and ubiquitination assays

Cell extracts were collected as previously described and incubated with primary antibodies to AKT (1:400), mTOR (1:200), LSD1 (1:200), ADH1A (1:400), CBL (1:200), or TRIM25 (1:500), and Protein G Sepharose beads (Santa Cruz Biotechnology, Santa Cruz, CA, USA). After the immunoprecipitates were washed 4 times, the target proteins were measured with Western blot, as previously described[28,29]. Antibodies targeting GPT2 (1:2,000), ADH1A (1:5,000), AKT (1:1,000), p-mTOR (1:500), LSD1 (1:2,000), mTOR (1:2,000), TRIM25 (1:2,000), FASN (1:1,000), SCD1 (1:2,000), HBsAg (1:400), β-tubulin (1:3,000), and GAPDH (1:5,000) were



Variable	HR	95% CI	*P* value
GPT2	0.66	0.47–0.94	0.02

Variable	HR	95% CI	*P* value
GPT2	0.87	0.62–1.22	0.42

Figure 1 GPT2 expression and clinical association with LC. (A) GPT2 protein expression in LC tissues and adjacent tissues, detected with IHC analysis. (B) Relative expression of GPT2 in TCGA LC cohorts. (C) Relative expression of GPT2 and associated statistical results in 7 LC cohorts from the HCCDB database. (D) Association of GPT2 with AFP levels in patients with LC in TCGA LC cohorts. (E) KM analysis of the association between GPT2 and OS in TCGA LC cohorts. (F) KM analysis of the association between GPT2 and DFS in TCGA LC cohorts. (G) Univariate

analyses of GPT2 expression for correlation with OS according to the Cox proportional hazards model. (H) Univariate analyses of GPT2 expression for correlation with DFS according to the Cox proportional hazards model. (I) Schoenfeld residual test on the proportional hazards assumption for GPT2 with OS. (J) Schoenfeld residual test on the proportional hazards assumption for GPT2 with DFS. Statistical analysis was performed with the chi-square test, *t*-test, and log-rank test. *P < 0.05, ***P < 0.001. AFP, alpha fetoprotein; DFS, disease-free survival; GPT2, glutamic-pyruvic transaminase 2; HCCDB, hepatocellular carcinoma database; IHC, immunohistochemistry; LC, liver cancer; OS, overall survival; TCGA, The Cancer Genome Atlas.

used for Western blot to determine protein expression levels. Protein G Sepharose beads and anti-ubiquitin antibodies (1:600) were used to detect ubiquitination. Western blot was performed to evaluate the ubiquitination of LSD1 (1:1,000) and GPT2 (1:2,000).

Statistical analysis

Differences in data values between 2 groups are expressed as means ± standard deviations (SDs) from at least 3 independent experiments, and were compared with the *t*-test. Differences among 3 or more groups were compared with one-way analysis of variance (ANOVA) (in which the least significant difference method was used to compare discrepancies between 2 groups). The significance of the correlations between various target proteins estimated by IHC was assessed with the chi-square test. The Kaplan–Meier (KM) method was used to examine the correlation of GPT2 expression with overall survival (OS) and disease-free survival (DFS), and differences were assessed with the log-rank test. Cox proportional hazards models were used to determine whether GPT2 expression was an independent prognostic factor. The results are presented as hazard ratios and corresponding 95% confidence intervals. In addition, the was verified with the Schoenfeld residuals test. The threshold for statistical significance was set at $P < 0.05$.

Results

GPT2 expression is significantly diminished in LC

To investigate the association between GPT2 and LC, we analyzed in-house clinical specimens and data from TCGA database. GPT2 expression was lower in LC tissues than adjacent normal tissues (**Figure 1A, B**). This finding was corroborated by analysis of 7 LC cohorts from the HCCDB database[36], which also demonstrated lower GPT2 expression in tumor tissues than adjacent non-tumor tissues (**Figure 1C**). Further analysis in TCGA cohort revealed an association between GPT2 expression and clinical parameters: GPT2 levels were lower in patients with LC with serum alpha fetoprotein (AFP) ≥ 20 ng/mL rather than < 20 ng/mL (**Figure 1D**). To further evaluate the clinical significance of GPT2, we divided patients into low- and high-expression groups according to median GPT2 expression. KM analysis with the log-rank test indicated that lower GPT2 expression was significantly associated with poorer OS but not DFS (**Figure 1E, F**). In addition, univariate Cox proportional hazards analysis identified low GPT2 expression as an independent prognostic factor for OS but not DFS (**Figure 1G, H**). Schoenfeld residual tests confirmed no violation of the proportional hazards assumption, thereby supporting the validity of the Cox models (**Figure 1I, J**). Together, these results indicated that low GPT2 expression significantly correlated with poor OS in patients with LC.

GPT2 inhibits the growth and migration of LC cells

We next assessed the effects of GPT2 on the proliferation and migration of LC cells. A plasmid for expression of Flag-tagged GPT2 was transfected into LC cells (**Figure S1A**). With CCK-8 and colony formation assays, we observed that GPT2 inhibited LC cell growth *in vitro* (**Figure S1B, C**). Transwell and wound healing assays (**Figure S1D, E**) further revealed that GPT2 overexpression decreased the migratory ability of LC cells. Additionally, in xenograft tumor models, GPT2 effectively suppressed tumor growth *in vivo*, according to measured tumor weight, volume, and expression of the proliferation marker Ki67 (**Figure S1F, G**). To further investigate GPT2 function, we generated a specific shRNA targeting GPT2. GPT2 knockdown (**Figure S1H**) promoted both LC cell growth and migration *in vitro* (**Figure S1I–L**). Moreover, GPT2 inhibition in nude mice enhanced tumor proliferation *in vivo* (**Figure S1M, N**). In summary, GPT2 was found to suppress malignant phenotypes in LC cells.

GPT2 regulates ADH1A expression in LC

GSEA was performed to further assess the biological processes associated with GPT2 in LC[41] in TCGA tumor cohorts[42]. A significant association was observed between GPT2 expression and fatty acid metabolism (**Figure 2A**). In agreement with this finding, analysis of the ARCHS[4] database[35] predicted GPT2's involvement in both fatty acid metabolism and degradation (**Figure 2B**). We evaluated fatty acid metabolism-related genes associated with GPT2 with GSEA (**Table S1**), and selected ADH1A for

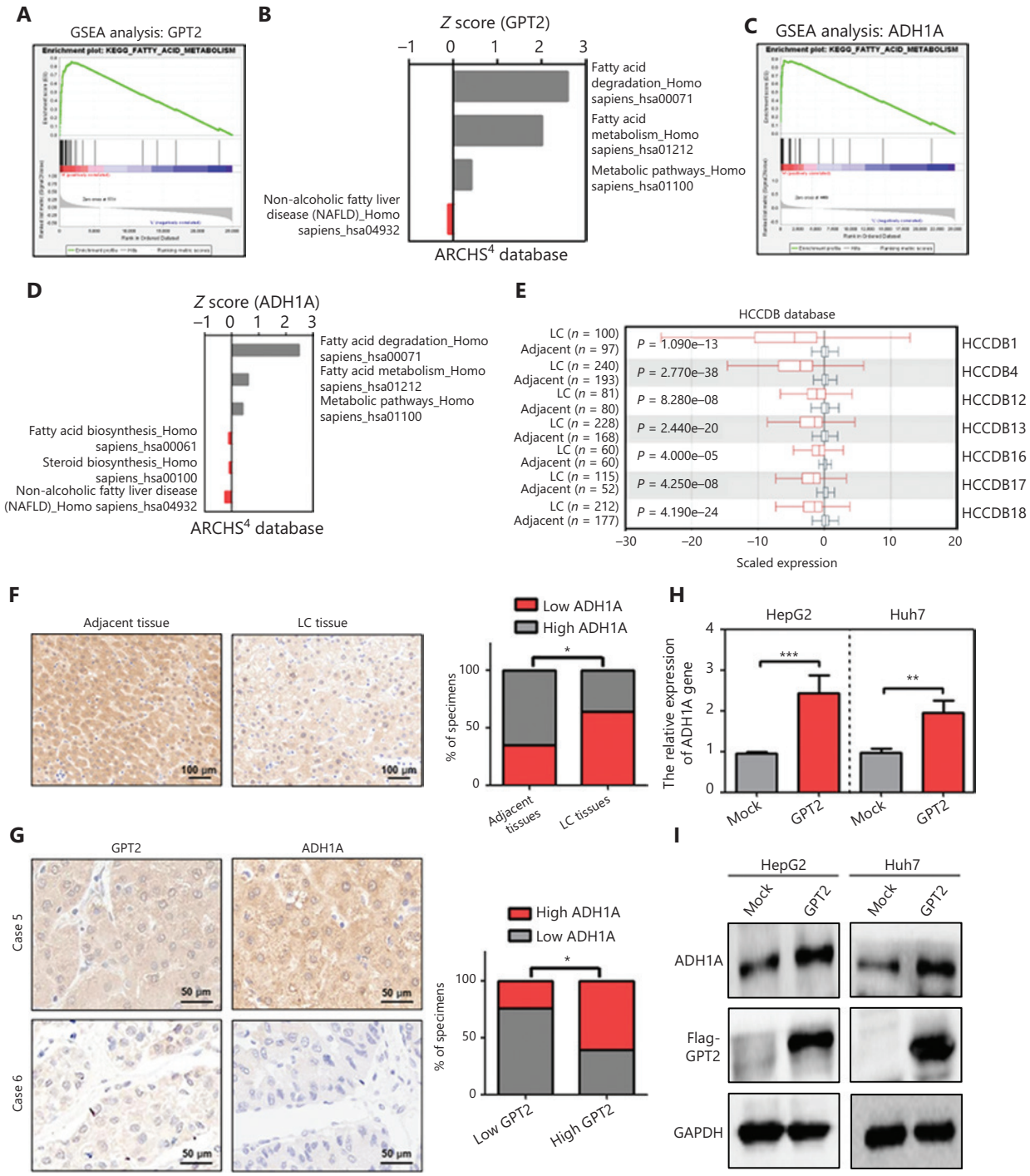


Figure 2 Effect of GPT2 on ADH1A expression in LC. (A) GSEA of pathways associated with GPT2, on the basis of TCGA LC cohort. (B) KEGG pathways associated with GPT2 in the ARCHS[4] database. (C) GSEA of pathways associated with ADH1A, on the basis of TCGA LC cohort. (D) KEGG pathways associated with ADH1A in the ARCHS[4] database. (E) Relative expression levels of ADH1A and associated statistical results in 7 LC cohorts from the HCCDB database. (F) ADH1A expression in LC tissues, detected with IHC. (G) Association of GPT2 with ADH1A in LC tissues, detected with IHC. (H) Effect of GPT2 on ADH1A gene expression, examined with real-time PCR. (I) Influence of GPT2 on ADH1A protein expression, evaluated with Western blot. Mock, LC cells transfected with control expression plasmids; GPT2, LC cells transfected with GPT2 expression plasmids. Statistical analysis was performed with chi-square test and *t*-test. **P* < 0.05, ***P* < 0.01, ****P* < 0.001. ADH1A, alcohol dehydrogenase 1A; GPT2, glutamic-pyruvic transaminase 2; GSEA, gene set enrichment analysis; HCCDB, hepatocellular carcinoma database; IHC, immunohistochemistry; LC, liver cancer; TCGA, The Cancer Genome Atlas.

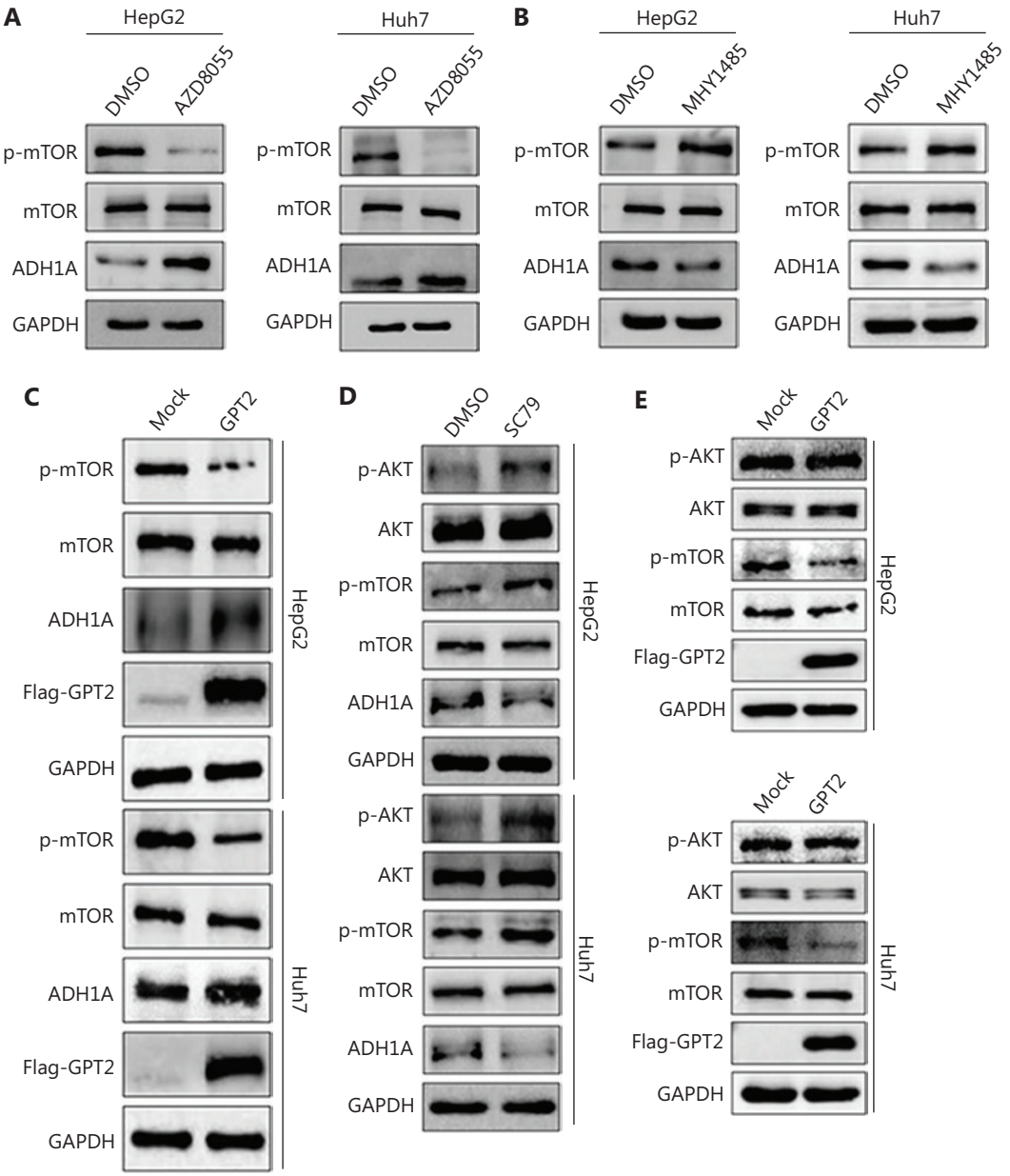


Figure 3 Continued

further investigation. A previous analysis of TCGA data by our group has indicated ADH1A downregulation in LC[13]. Herein, ADH1A was similarly associated with fatty acid metabolism and degradation (**Figure 2C, D**) and therefore might be an important downstream target of GPT2 in modulating lipid metabolism.

Analysis of the HCCDB database revealed diminished ADH1A expression in LC (**Figure 2E**) within the same cohorts (**Figure 1C**). IHC staining further demonstrated lower ADH1A expression in tumor tissues than adjacent normal tissues (**Figure 2F**). Moreover, we observed a significant positive correlation between GPT2 and ADH1A expression in LC tissues (**Figure 2G**). Using LC cell models, we evaluated the effect of GPT2 on ADH1A and observed that exogenous GPT2 increased ADH1A expression (**Figure 2H, I**). Together, these results highlighted the critical role of GPT2 in regulating ADH1A expression in LC.

We also examined whether ADH1A might be involved in GPT2-mediated regulation of LC cell behavior. Although GPT2 silencing promoted LC cell growth and migration, these effects were reversed by the addition of exogenous ADH1A (**Figure S2**). Therefore, ADH1A was determined to contribute to the inhibitory effects of GPT2 on LC cell growth and migration.

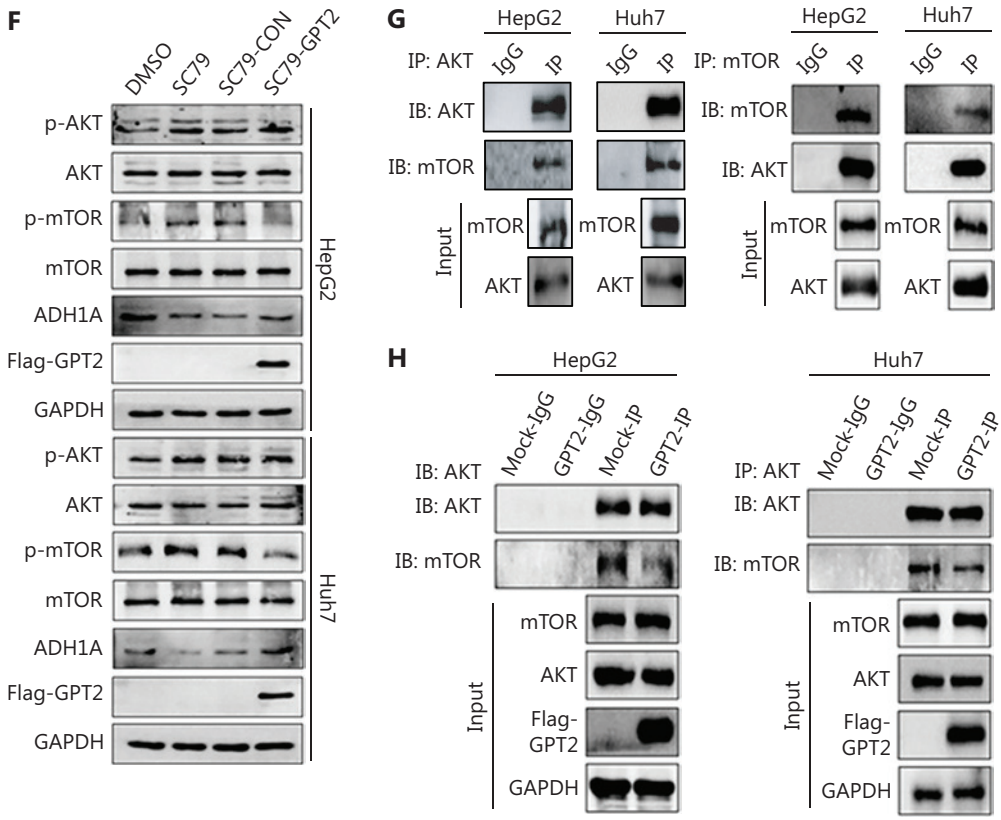


Figure 3 Influence of GPT2 on mTOR signaling pathway activation and regulation of ADH1A expression. (A) Effects of inhibition of mTOR with AZD8055 on ADH1A expression in LC cells. (B) Effects of activation of mTOR with MHY1485 on ADH1A expression in LC cells. (C) Effects of GPT2 on mTOR activation and ADH1A expression in LC cells. (D) Effects of AKT activation mediated by the activator SC79 on mTOR sensitization and ADH1A expression in LC cells. (E) Effects of GPT2 on the activation of AKT and mTOR in LC cells. (F) Effects of GPT2 on mTOR activation and ADH1A expression mediated by AKT activation in LC cells. (G) AKT–mTOR interaction, assessed with co-IP assays. (H) Effects of GPT2 on AKT–mTOR interaction, measured with co-IP assays in LC cells. ADH1A, alcohol dehydrogenase 1A; AKT, protein kinase B; co-IP, co-immunoprecipitation; GPT2, glutamic-pyruvic transaminase 2; LC, liver cancer; mTOR, mammalian target of rapamycin.

GPT2 suppresses the mTOR signaling pathway and consequently upregulates ADH1A

Next, we assessed the mechanism through which GPT2 modulates ADH1A expression. Given that the mTOR signaling pathway inhibits ADH1A[14], we evaluated its role in regulating ADH1A expression in LC cells treated with the mTOR inhibitor AZD8055 and activator MHY1485. mTOR inhibition increased ADH1A expression, whereas mTOR activation decreased ADH1A levels (**Figure 3A, B**). Analysis of the ARCHS[4] database suggested a potential interaction between GPT2 and mTOR (**Figure S3A**). Therefore, we examined whether GPT2 might regulate ADH1A *via* the mTOR pathway. Co-immunoprecipitation (co-IP) and immunofluorescence assays confirmed that GPT2 interacted and colocalized with mTOR in tumor cells (**Figure S3B, C**). We further generated GPT2 mutants containing or lacking aminotransferase class I/II domains (GPT2-1 and GPT2-2, respectively). The finding that GPT2-1 mutant, which retained these domains, interacted with mTOR indicated that aminotransferase domains are necessary for the GPT2–mTOR interaction (**Figure S3D–F**).

Additionally, to determine which regions of mTOR bind GPT2, we constructed and expressed mTOR mutants with C-terminal, double-terminal, and N-terminal deletions (**Figure S3G, H**). Co-IP assays revealed that the double-terminal deletion mutant of mTOR interacted with GPT2, thereby suggesting that the central region of mTOR mediates its binding GPT2 (**Figure S3I**). Furthermore, GPT2 suppressed mTOR sensitization and promoted ADH1A upregulation (**Figure 3C**).

Subsequently, we investigated the mechanism through which GPT2 inhibited mTOR in regulating ADH1A expression. Given that AKT, a key kinase in the PI3-K pathway, enhances mTOR sensitization[43], we used the AKT activator SC97 to examine the involvement of AKT in mTOR sensitization in the regulation of ADH1A. AKT activation enhanced mTOR sensitization and suppressed ADH1A expression in LC cells (**Figure 3D**). We next tested whether GPT2 might

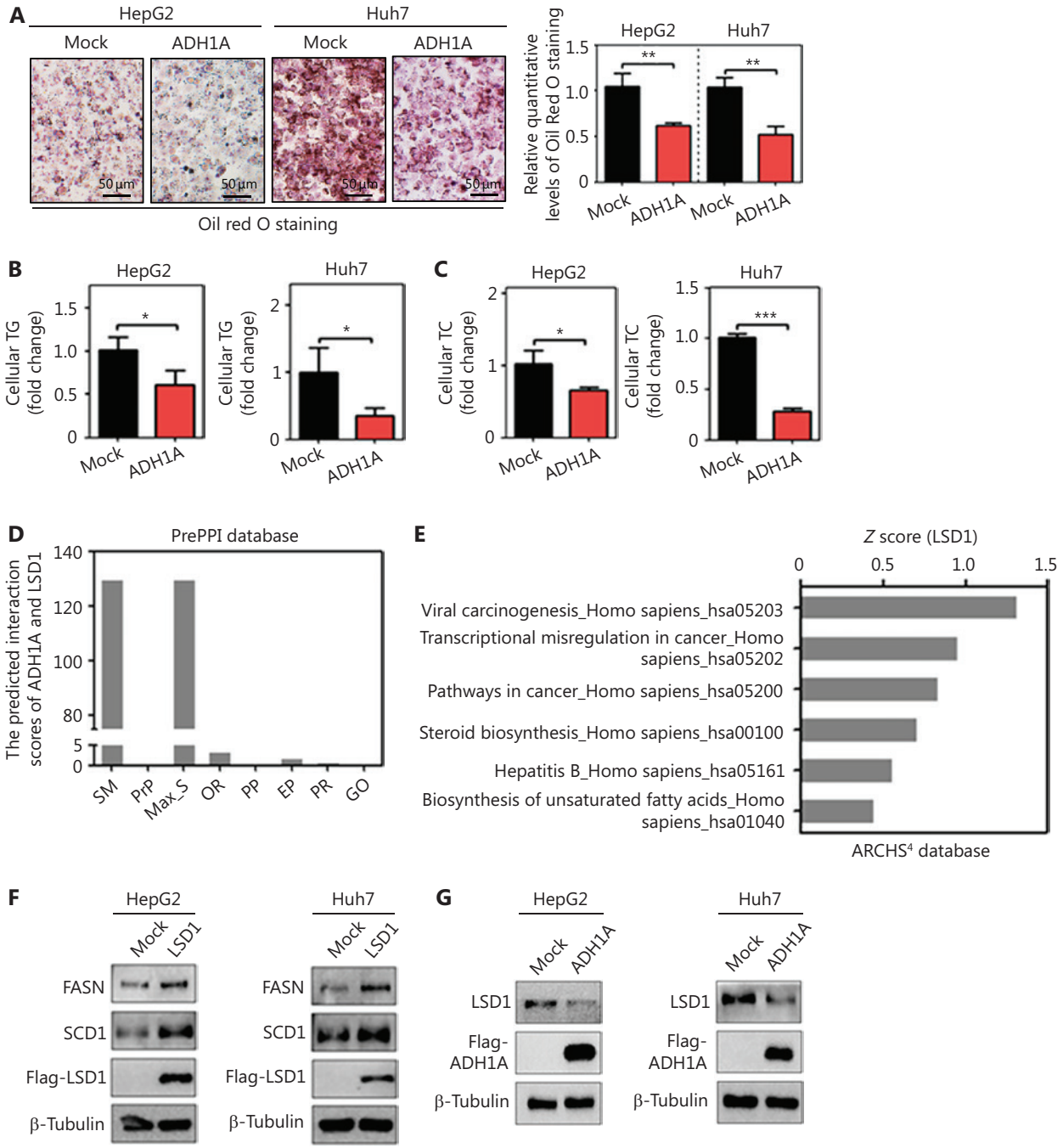


Figure 4 Continued

influence mTOR *via* AKT. Although GPT2 did not alter AKT activation (**Figure 3E**), it impaired AKT-mediated mTOR sensitization (**Figure 3F**). Because GPT2 disrupted the binding between AKT and mTOR (**Figure 3G, H**), we concluded that decreased AKT-mTOR interaction contributed to GPT2-induced mTOR inhibition and subsequent ADH1A modulation in LC cells.

We also assessed whether GPT2 enzymatic activity might be necessary for mTOR pathway regulation. Mutations in the aminotransferase domains (C259R, N271T, and V478R; **Figure S4A**)[31] impair GPT2 activity. A mutant GPT2 plasmid (GPT2-Mut) carrying these mutations was therefore transfected into LC cells. Co-IP assays revealed that GPT2-Mut weakened the GPT2–mTOR interaction (**Figure**

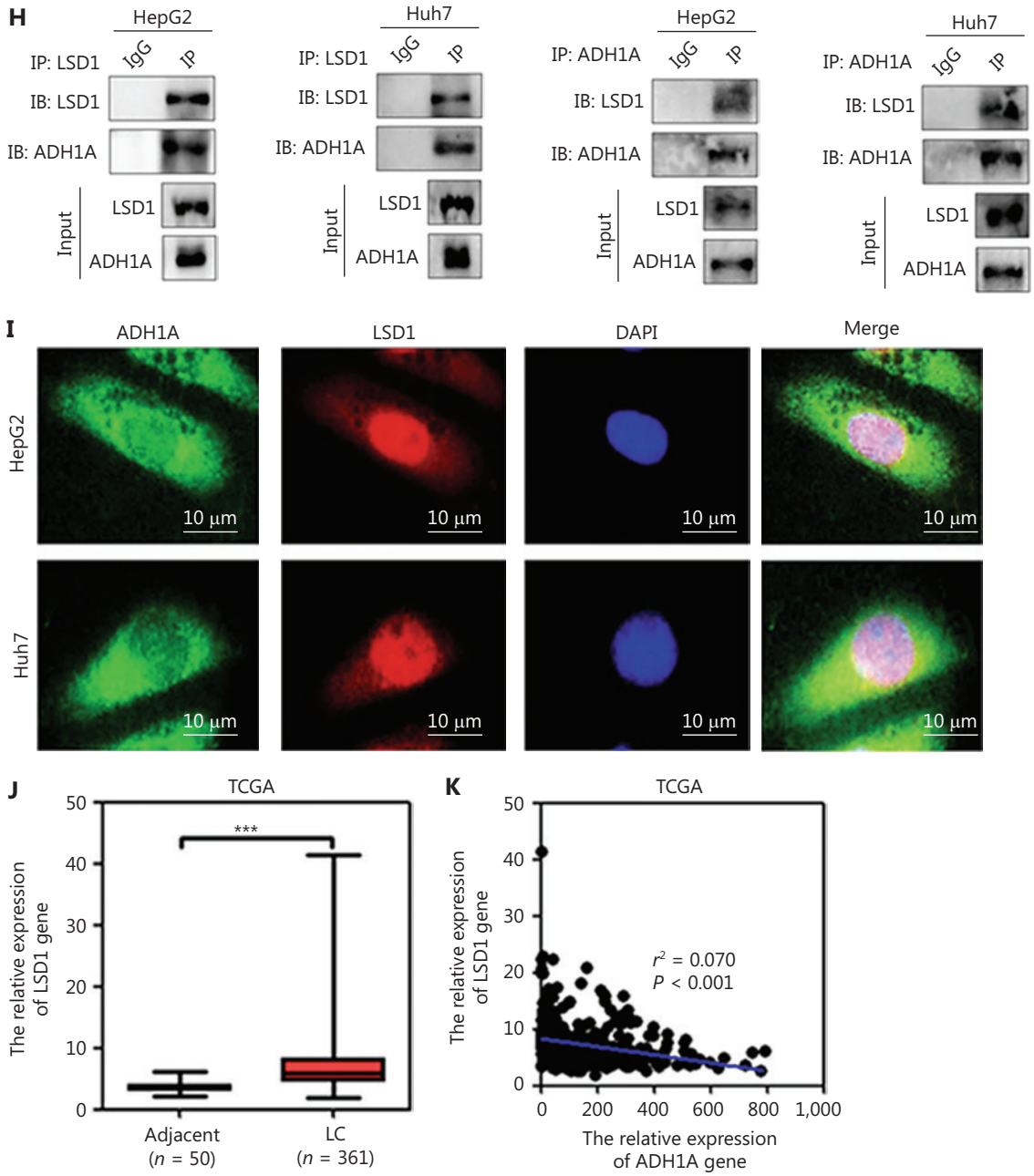


Figure 4 Continued

S4B) but enhanced mTOR–AKT binding (**Figure S4C**). Although, as previously shown, wild-type GPT2 inhibited mTOR and consequently upregulated ADH1A, mTOR activity was restored, and ADH1A expression was diminished, in cells expressing the enzymatically impaired GPT2 mutant (**Figure S4D**). Therefore, overall, GPT2-mediated regulation of mTOR and ADH1A might depend on its enzymatic activity.

ADH1A facilitates decreased LSD1 expression and lipid accumulation mediated by GPT2 in LC cells

Although ADH1A might be involved in fatty acid metabolism, a process essential for hepatic lipid synthesis (**Figure 2C, D**)[44], its specific role in LC remains unclear. Oil Red O staining and measurements of TC and TG levels indicated that ADH1A

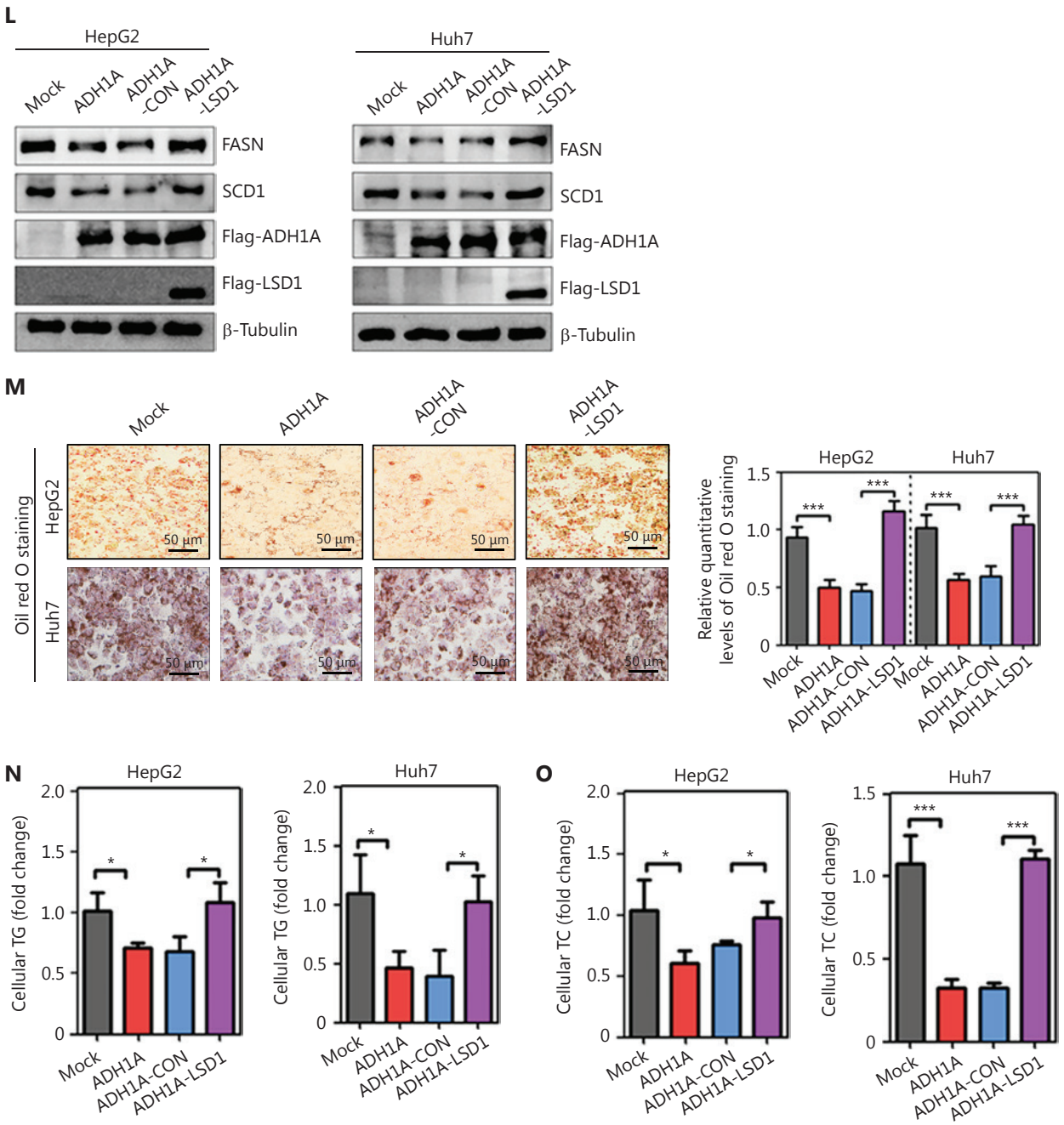


Figure 4 Effects of ADH1A and GPT2 on LSD1 expression and lipid accumulation in LC. (A) Effect of ADH1A on lipid droplet accumulation, detected with Oil Red O staining. (B) Influence of ADH1A on triglyceride content in LC cells. (C) Effect of ADH1A on cholesterol content in LC cells. (D) Interaction between ADH1A and LSD1, predicted with the PrePPI database. (E) Predicted KEGG pathways relevant to LSD1 in the ARCHS[4] database. (F) Influence of LSD1 on FASN and SCD1 expression in LC cells. (G) Influence of ADH1A on LSD1 expression in LC cells. (H) Interaction of ADH1A with LSD1, evaluated with co-IP assays. (I) Colocalization between ADH1A and LSD1, detected with immunofluorescence assays. (J) LSD1 gene expression in TCGA LC cohort. (K) Relationship between ADH1A and the LSD1 gene in TCGA LC cohort. (L) Effects of LSD1 on FASN and SCD1 expression mediated by ADH1A. (M) Effect of LSD1 on lipid droplets mediated by ADH1A. (N) Effect of LSD1 on triglyceride content mediated by ADH1A. (O) Effect of LSD1 on total cholesterol content mediated by ADH1A. Mock, LC cells transfected with control expression plasmids; ADH1A, LC cells transfected with ADH1A expression plasmids; ADH1A-CON, ADH1A-positive LC cells transfected with control expression plasmids; ADH1A-LSD1, ADH1A-positive LC cells transfected with LSD1 expression plasmids. Statistical analysis was performed with *t*-test and one-way ANOVA. **P* < 0.05, ***P* < 0.01, ****P* < 0.001. ADH1A, alcohol dehydrogenase 1A; ANOVA, analysis of variance; GPT2, glutamic-pyruvic transaminase 2; LC, liver cancer; LSD1, lysine-specific demethylase 1; TCGA, The Cancer Genome Atlas.

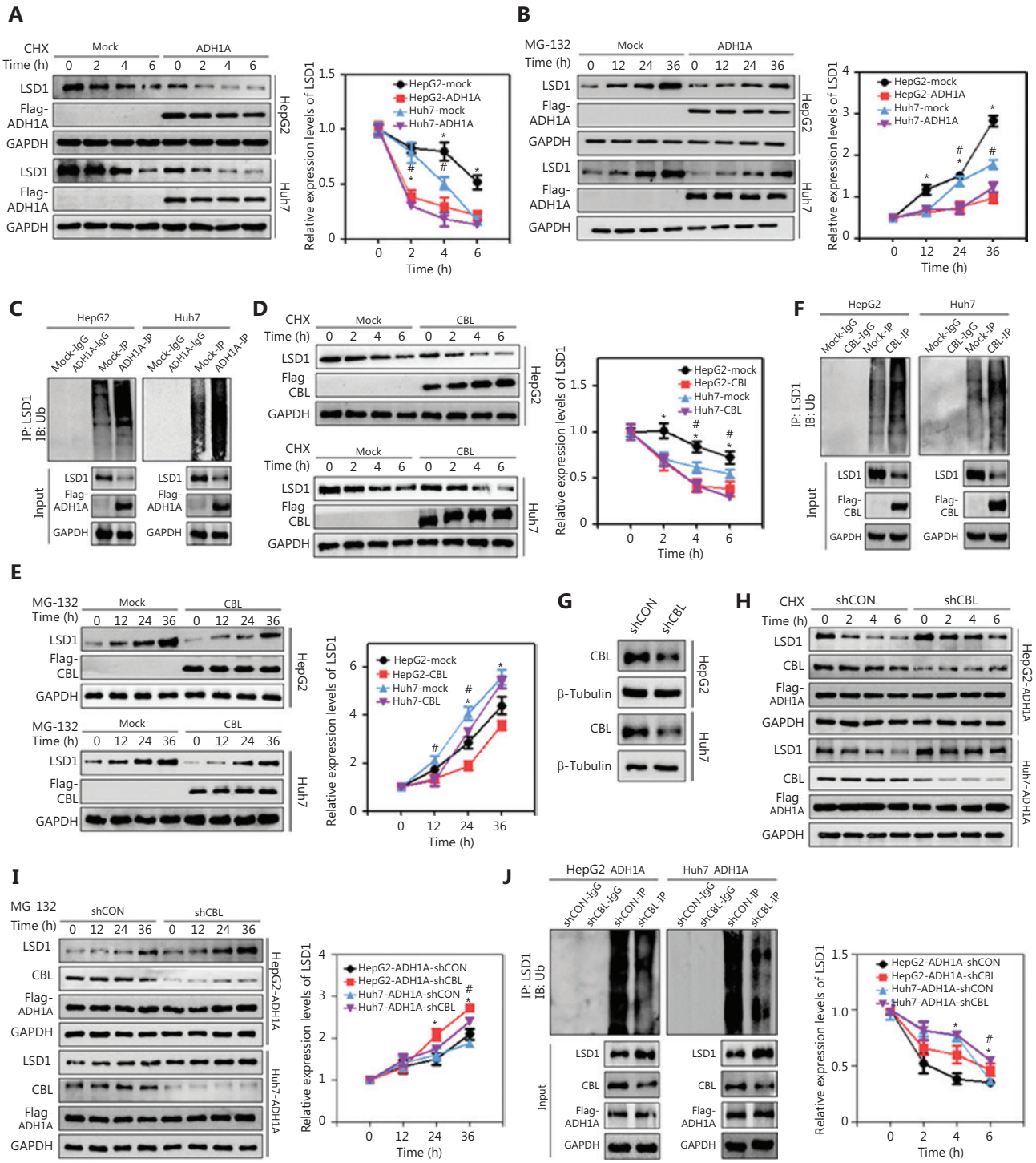


Figure 5 Inhibition of LSD1 stabilization mediated by ADH1A *via* CBL. (A) Effect of ADH1A on LSD1 stabilization after treatment of LC cells with CHX (200 μg/mL) to inhibit protein synthesis. **P* < 0.05, mock *vs.* ADH1A group in HepG2 cells; #*P* < 0.05, mock *vs.* ADH1A group in Huh7 cells. (B) Influence of ADH1A on LSD1 stabilization after treatment of LC cells with the proteasome inhibitor MG-132 (100 nM). **P* < 0.05, mock *vs.* ADH1A group in HepG2 cells; #*P* < 0.05, mock *vs.* ADH1A group in Huh7 cells. (C) Influence of ADH1A on LSD1 ubiquitination in LC cells. (D) Effect of CBL on LSD1 stabilization after treatment of LC cells with CHX (200 μg/mL) to inhibit protein synthesis. **P* < 0.05, mock *vs.* CBL group in HepG2 cells; #*P* < 0.05, mock *vs.* CBL group in Huh7 cells. (E) Influence of CBL on LSD1 stabilization after treatment of LC cells with the proteasome inhibitor MG-132 (100 nM). **P* < 0.05, mock *vs.* CBL group in HepG2 cells; #*P* < 0.05, mock *vs.* CBL group in Huh7 cells. (F)

Influence of CBL on LSD1 ubiquitination in LC cells. (G) Inhibition of CBL protein expression with a specific shRNA. (H) Effect of CBL on LSD1 stabilization mediated by ADH1A after treatment of LC cells with CHX (200 μg/mL) to inhibit protein synthesis. *P < 0.05, mock *vs.* ADH1A-shCON group in HepG2 cells; #P < 0.05, mock *vs.* ADH1A-shCBL group in Huh7 cells. (I) Influence of CBL on LSD1 stabilization mediated by ADH1A after treatment of LC cells with the proteasome inhibitor MG-132 (100 nM). *P < 0.05, mock *vs.* ADH1A-shCON group in HepG2 cells; #P < 0.05, mock *vs.* ADH1A-shCBL group in Huh7 cells. (J) Effect of CBL on LSD1 ubiquitination mediated by ADH1A in LC cells. ADH1A, LC cells transfected with ADH1A expression plasmids; CBL, LC cells transfected with CBL expression plasmids; mock, LC cells transfected with control plasmids; shCON, LC cells transfected with shRNA control plasmids; shCBL, LC cells transfected with shRNA-targeting CBL plasmids. Statistical analysis was performed with *t*-test. ADH1A, alcohol dehydrogenase 1A; CBL, casitas B lineage lymphoma; CHX, cycloheximide; LC, liver cancer; LSD1, lysine-specific demethylase 1.

suppressed lipid accumulation in LC cells (**Figure 4A–C**). To elucidate the mechanism through which ADH1A modulates lipid storage, we consulted the PrePPI database[38], and identified a potential interaction between ADH1A and LSD1 (**Figure 4D**), a histone demethylase that promotes lipid synthesis by upregulating key lipogenic enzymes[45]. Additionally, data from the ARCHS[4] database associated LSD1 with steroid biosynthesis, unsaturated fatty acid biosynthesis, and cancer-related pathways (**Figure 4E**). LSD1 therefore might potentially contribute to hepatocarcinogenesis by regulating ADH1A-mediated lipid accumulation.

Because LSD1 upregulates the expression of lipogenic genes SCD1 and FASN[45], we examined its effects on these molecules in LC cells. LSD1 markedly increased the expression of SCD1 and FASN (**Figure 4F**). Moreover, ADH1A suppressed LSD1 expression (**Figure 4G**). Co-IP and immunofluorescence assays confirmed the interaction and colocalization of LSD1 and ADH1A (**Figure 4H, I**). In TCGA cohorts, LSD1 expression was higher in LC tissues than adjacent tissues but was negatively correlated with ADH1A levels (**Figure 4J, K**). We further demonstrated that ADH1A overexpression repressed FASN and SCD1 expression in LC cells. However, transfection of exogenous LSD1 into ADH1A-overexpressing LC cells restored the expression of FASN and SCD1 (**Figure 4L**). In contrast, knockdown of ADH1A with a specific shRNA upregulated FASN and SCD1 expression; however, this expression was inhibited when LSD1 was silenced in ADH1A-deficient cells (**Figure S5**). Additionally, assessments of lipid droplets, TC, and TG revealed that ADH1A overexpression suppressed lipid accumulation in LC cells, but this effect was reversed by ectopic LSD1 treatment (**Figure 4M–O**).

More importantly, we examined whether GPT2 might regulate LSD1, FASN, and SCD1 expression, as well as lipid accumulation in LC cells *via* ADH1A. In agreement with our prediction, GPT2 silencing elevated LSD1, FASN, and SCD1 levels, and increased lipid accumulation in LC cells, on the basis of lipid droplets, TG, and TC (**Figure S6**). However, when ectopic ADH1A was transfected, the GPT2 deficiency-induced upregulation of LSD1, FASN, and SCD1, and the enhanced lipid accumulation were suppressed.

CBL is crucial for ADH1A-mediated inhibition of LSD1 stabilization

Although ADH1A inhibits LSD1 expression through direct interactions, the underlying mechanisms remain unclear. Given that protein interactions can regulate target protein stability *via* the ubiquitin–proteasome system[46], we investigated whether ADH1A might affect LSD1 stabilization. In agreement with our hypothesis, treatment of ADH1A overexpressing LC cells with the protein synthesis inhibitor CHX, or the proteasome inhibitor MG-132 significantly decreased the half-life and stability of LSD1 (**Figure 5A, B**). Furthermore, ADH1A enhanced LSD1 ubiquitination in LC (**Figure 5C**).

ADH1A decreased LSD1 stability in a ubiquitin–proteasome-dependent manner. However, ADH1A is not an E3 ubiquitin ligase capable of directly ubiquitinating target proteins. Analysis of the UbiBrowser database[39] predicted CBL as the highest-scoring potential E3 ligase for LSD1 (**Figure S7A**). In agreement with this finding, CBL suppressed LSD1 expression in LC (**Figure S7B**). Co-IP and immunofluorescence assays confirmed the physical interaction and colocalization of CBL with LSD1 (**Figure S7C, D**). Moreover, CBL significantly shortened the half-life and decreased the stability of LSD1 (**Figure 5D, E**), whereas ectopic expression of CBL in LC cells enhanced LSD1 ubiquitination (**Figure 5F**). Collectively, these results established CBL as a key E3 ubiquitin ligase for LSD1 in LC cells.

We further investigated whether CBL might be required for ADH1A-mediated inhibition of LSD1. In LC cells, ADH1A increased CBL protein levels and interacted with CBL (**Figure S8A, B**). More importantly, ADH1A enhanced the interaction between CBL and LSD1 (**Figure S8C**); therefore, we reasoned that CBL might be involved in ADH1A-induced suppression of LSD1. To test this hypothesis, we constructed an shRNA plasmid targeting CBL (**Figure 5G**). Silencing CBL in ADH1A-overexpressing LC cells significantly extended the half-life and increased the stability of LSD1 (**Figure 5H, I**), while decreasing its ubiquitination level (**Figure 5J**). Overall, ADH1A promotes the ubiquitination of LSD1 *via* CBL, thereby inhibiting its stabilization.

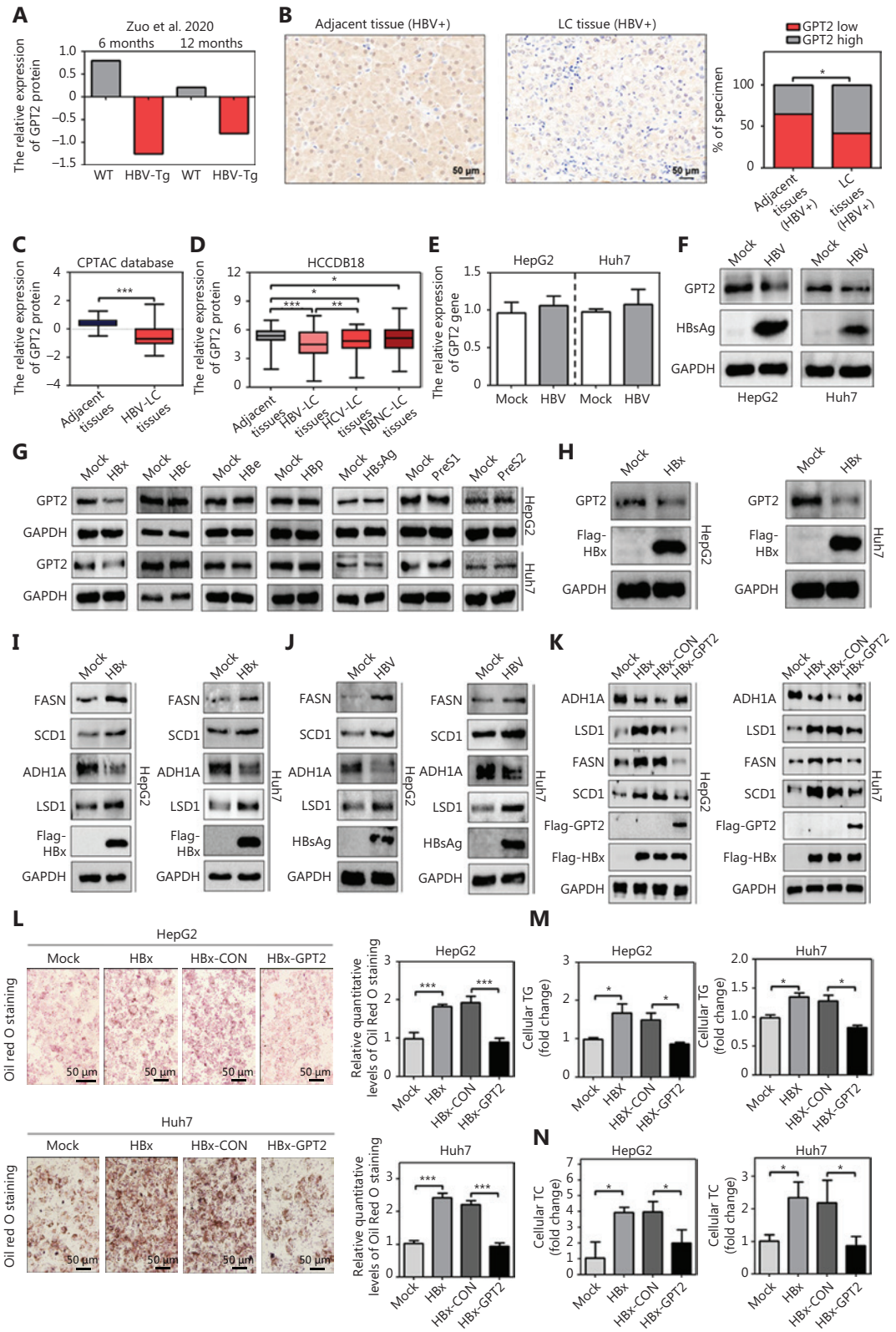


Figure 6 Effects of HBx on GPT2 expression in LC cells. (A) Effect of HBV on GPT2 protein expression in HBV-Tg mice. (B) GPT2 expression in HBV-positive (HBV+) adjacent tissues and HBV+ tumor tissues, detected with IHC. (C) GPT2 expression in HBV-positive LC tissues and adjacent tissues from the CPTAC database. (D) GPT2 expression in HBV-positive LC tissues, hepatitis C virus (HCV)-associated LC,

non-HBV-HCV-associated LC tissues, and adjacent tissues from the HCCDB18 cohort. (E) Effect of HBV on GPT2 gene expression in LC cells, assessed with real-time PCR. (F) Role of HBV in GPT2 protein expression in LC cells, examined with western blotting. (G) Influence of transient transfection of various HBV genes on GPT2 protein expression. (H) Effect of stable HBx transfection on GPT2 protein expression. (I) Effects of HBx on ADH1A, FASN, SCD1, and LSD1 expression. (J) Effects of HBV on ADH1A, FASN, SCD1, and LSD1 expression. (K) Effects of GPT2 on ADH1A, FASN, SCD1, and LSD1 expression mediated by HBx. (L) Effect of GPT2 on lipid droplets mediated by HBx. (M) Effect of GPT2 on triglyceride content mediated by HBx. (N) Effect of GPT2 on cholesterol content mediated by HBx. WT, wild-type mice; HBV Tg, HBV transgenic mice; mock, LC cells transfected with control plasmids; HBV, LC cells transfected with HBV expression plasmids; HBx, LC cells transfected with HBx expression plasmids; HBx-CON, HBx-positive LC cells transfected with control expression plasmids; HBx-GPT2, HBx-positive LC cells transfected with GPT2 expression plasmids. Statistical analysis was performed with *t*-test and one-way ANOVA. $*P < 0.05$, $**P < 0.01$, $***P < 0.001$. ADH1A, alcohol dehydrogenase 1A; ANOVA, analysis of variance; FASN, fatty acid synthase; GPT2, glutamic-pyruvic transaminase 2; HBV, hepatitis B virus; HBX, hepatitis B virus X protein; HCV, hepatitis C virus; LC, liver cancer; LSD1, lysine-specific demethylase 1; PCR, polymerase chain reaction; SCD1, stearoyl-CoA decarboxylase 1; TC, total cholesterol; TG, triglyceride.

HBx decreases GPT2 expression, thus leading to lipid accumulation in LC cells

HBV infection is a significant risk factor for LC. On the basis of the proteomic data reported by Zuo et al.[47], we identified lower GPT2 protein levels in HBV-transgenic mice (**Figure 6A**). Therefore, we detected whether HBV might similarly suppress GPT2 expression in human LC. IHC analysis revealed lower GPT2 expression in HBV-associated LC tissues than adjacent non-tumor tissues (**Figure 6B**). This finding was further confirmed in HBV-positive tumor tissue data from the CPTAC database[37] (**Figure 6C**). Analysis of the HCCDB18 cohort indicated lower GPT2 expression in LC tissues associated with HBV, hepatitis C virus (HCV), and non-HBV/non-HCV etiologies than in adjacent tissues; therefore, multiple pathogenic factors appeared to downregulate GPT2 in tumors. Among these, GPT2 expression was lowest in HBV-associated LC and was significantly lower in HBV-associated LC than HCV-positive LC (**Figure 6D**). Overall, HBV might play a prominent role in suppressing GPT2 expression in LC. Next, using LC cell models, we demonstrated that HBV inhibited GPT2 protein expression (**Figure 6E, F**). Among viral genes, HBx, whether transiently or stably expressed, was responsible for this suppression (**Figure 6G, H**).

In LC cells, we also observed that HBx downregulated ADH1A, and upregulated LSD1, FASN, and SCD1 (**Figure 6I**). Similar effects were observed in the full HBV infection group (**Figure 6J**). GPT2 repression in HBx-positive cells decreased ADH1A expression, and increased LSD1, FASN, and SCD1 expression (**Figure 6K**). Furthermore, we confirmed that HBx promoted lipid accumulation in LC cells by inhibiting GPT2 (**Figure 6L–N**).

HBx downregulates GPT2, thus facilitating LC cell growth and migration

We next examined the effects of GPT2 on HBx-mediated cell proliferation and migration. HBx enhanced the growth of LC cells. However, after transfection of exogenous GPT2 into HBx-positive cells, this proliferative effect was suppressed (**Figure S9A, B**). Similarly, HBx promoted LC cell migration, whereas this effect was reversed by ectopic expression of GPT2 (**Figure S9C, D**). In a subcutaneous xenograft model, HBx facilitated tumor formation. *In vivo*, exogenous GPT2 treatment of HBx-positive LC cells abrogated the HBx-induced increase in tumor growth, on the basis of tumor weight, volume, and Ki67 expression in tumor tissues (**Figure S9E, F**).

TRIM25 is involved in the suppression of GPT2 stabilization mediated by HBx

HBx plays a critical role in modulating the stabilization of target proteins *via* ubiquitination, thus facilitating LC development[48]. To determine whether HBx might affect GPT2 stabilization, we treated LC cells with CHX and MG-132. HBx significantly decreased the half-life and stability of GPT2 (**Figure S10A, B**) and increased its ubiquitination levels in tumor cells (**Figure S10C**).

Given that HBx regulates target protein stabilization through specific E3 ligases[48], we sought to identify the E3 ligases involved in HBx-mediated GPT2 destabilization. Using the UbiBrowser database[39], we predicted potential E3 ligases for GPT2, among which CBL, NEDD4, and TRIM25 ranked highest (**Figure 7A**). We then evaluated the effects of these E3 ligases on GPT2 and found that TRIM25 markedly suppressed GPT2 expression (**Figure 7B**). Immunofluorescence and co-IP assays confirmed that TRIM25 colocalized and interacted with GPT2 (**Figure 7C, D**). Further experiments demonstrated that TRIM25 decreased the half-life and stability of GPT2 by promoting its ubiquitination (**Figure 7E-G**).

In line with our previous report[28], HBx did not substantially affect TRIM25 expression but was found to bind TRIM25 (**Figure S11A, B**). Co-IP additionally verified the interaction between HBx and GPT2 in LC (**Figure S11C**). Using previously constructed HBx deletion mutants (HBx1: C-terminal deletion; HBx2: double-terminal deletion; and HBx3: N-terminal deletion)[49] (**Figure S11D**), we observed that HBx interacted with TRIM25 and GPT2 *via* distinct regions (**Figure S11E**).

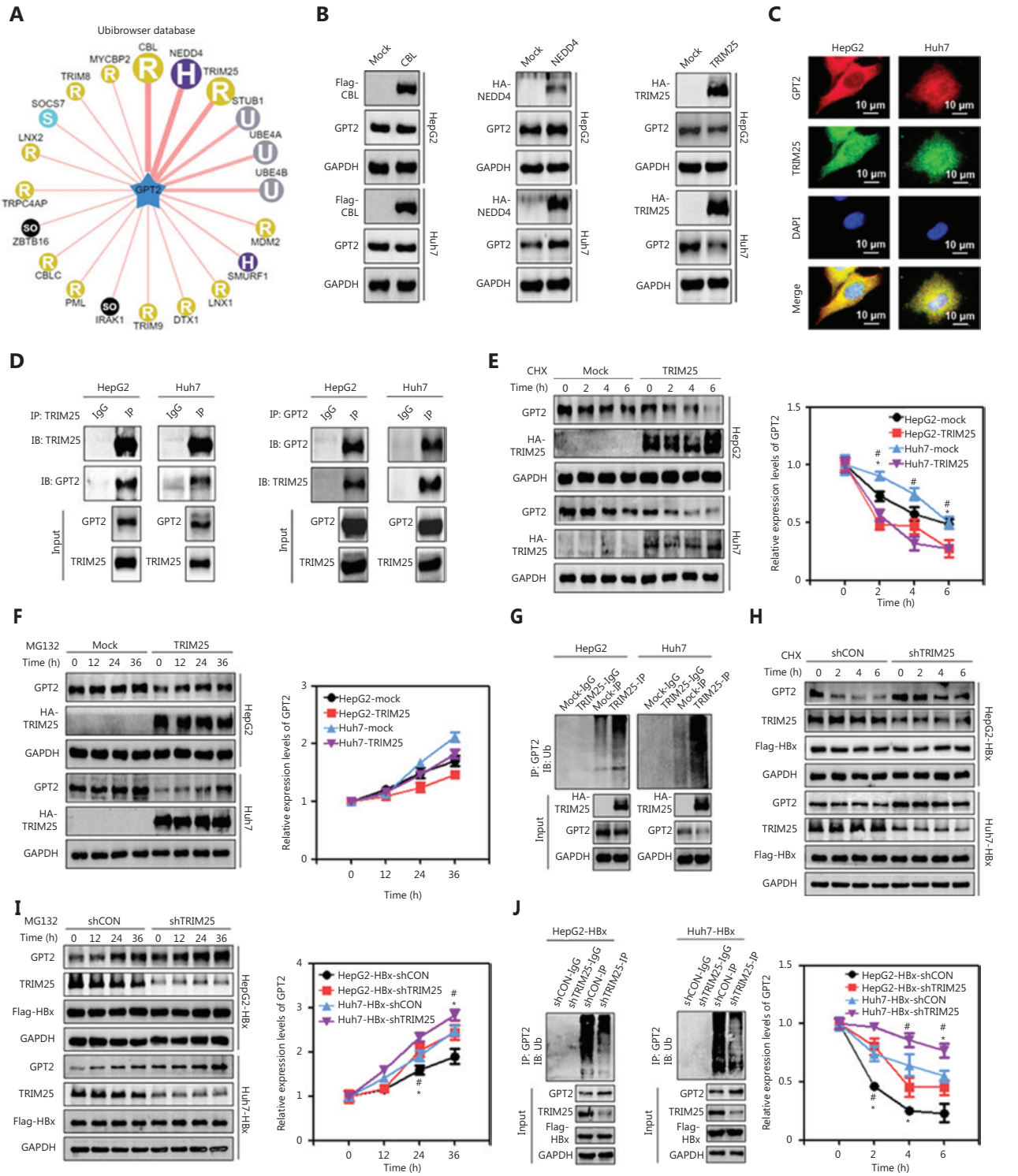


Figure 7 Regulation of GPT2 stabilization mediated by HBx *via* TRIM25. (A) Predicted E3 ligases of GPT2 in the UbiBrowser online database. (B) Influence of CBL, NEDD4, and TRIM25 on GPT2 expression. (C) Colocalization of TRIM25 with GPT2, examined with immunofluorescence. (D) Interaction of TRIM25 with GPT2, evaluated with Co-IP assays. (E) Effect of TRIM25 on GPT2 stabilization after treatment of LC cells with CHX (200 μg/mL) to inhibit protein synthesis. **P* < 0.05, mock *vs.* TRIM25 group in HepG2 cells; #*P* < 0.05, mock *vs.* TRIM25 group in Huh7 cells. (F) Effect of TRIM25 on GPT2 stabilization after treatment of LC cells with the proteasome inhibitor MG-132 (100 nM). (G) Effect of TRIM25 on GPT2 ubiquitination in LC cells. (H) Effect of TRIM25 on GPT2 stabilization mediated by HBx after treatment of LC cells with CHX (200 μg/mL)

to inhibit protein synthesis. *P < 0.05, shCON *vs.* shTRIM25 group in HepG2-HBx cells; #P < 0.05, shCON *vs.* shTRIM25 group in Huh7-HBx cells. (I) Effect of TRIM25 on GPT2 stabilization mediated by HBx after treatment of LC cells with the proteasome inhibitor MG-132 (100 nM). *P < 0.05, shCON *vs.* shTRIM25 group in HepG2-HBx cells; #P < 0.05, shCON *vs.* shTRIM25 group in Huh7-HBx cells. (J) Influence of TRIM25 on GPT2 ubiquitination mediated by HBx in LC cells. CBL, LC cells transfected with CBL expression plasmids; NEDD4, LC cells transfected with NEDD4 expression plasmids; shCON, LC cells transfected with shRNA control plasmids; shTRIM25, LC cells transfected with TRIM25 shRNA plasmids; TRIM25, LC cells transfected with TRIM25 expression plasmids. Statistical analysis was performed with *t*-test. CHX, cycloheximide; co-IP, co-immunoprecipitation; GPT2, glutamic-pyruvic transaminase 2; HBx, hepatitis B virus X protein; LC, liver cancer; TRIM25, tripartite motif containing 25.

Moreover, HBx functioned as an adaptor strengthening the association between GPT2 and TRIM25 (**Figure S11F**). Therefore, HBx promoted GPT2 ubiquitination and destabilization in a TRIM25-dependent manner. In agreement with this finding, TRIM25 knockdown in HBx-expressing LC cells abolished the HBx-mediated decrease in GPT2 stability and the increase in GPT2 ubiquitination (**Figure 7H–J**).

Discussion

LC remains a lethal disease. Although advances in clinical management have improved patient survival, curative options remain limited. Therefore, identifying factors that promote malignancy is critical for identifying novel therapeutic targets. Herein, we demonstrated that GPT2 was downregulated in LC, and its deficiency decreased ADH1A levels, and consequently increased LSD1 expression and lipid accumulation. We further demonstrated that HBV suppressed GPT2 expression in tumors *via* HBx. HBx was found to promote lipid storage, as well as LC cell proliferation and migration, by inhibiting GPT2. Moreover, TRIM25 facilitated HBx-mediated destabilization of GPT2 (**Figure 8**).

GPT2 is aberrantly expressed in multiple cancers, and it participates in various biological processes, such as glutamine metabolism, glycolysis, proliferation, and metastasis[5-7,50]. However, its expression pattern varies across tumor types[6,7,51,52]. For example, GPT2 is downregulated in glioblastoma[52], but upregulated in breast and bladder cancers[7,8]. However, the clinical relevance and functional role of GPT2 in LC remain unclear. Herein, analyses of our cohort, as well as TCGA and HCCDB cohorts, revealed diminished GPT2 levels in LC, in agreement with findings from Ji et al.[51] indicating diminished GPT2 expression in LC tissues and cell lines. Moreover, we observed that low GPT2 expression was associated with poor survival in patients with LC. Interestingly, because GPT2 correlated with poor OS but not DFS, it might not effectively predict prognosis after interventional therapy. In addition, *in vitro* and *in vivo* functional studies confirmed that GPT2 suppresses LC cell proliferation and migration, and therefore has a tumor-suppressive role in LC.

The liver synthesizes fatty acids and cholesterol, and dysregulated lipid metabolism influences LC prognosis by affecting signaling, the immune microenvironment, and processes such as survival, growth, and metastasis[53,54]. However, the mechanisms regulating lipid metabolism in LC are unclear. Herein, GSEA indicated associations between GPT2 and both fatty acid metabolism and diminished lipid accumulation. ADH1A was identified as a downstream target of GPT2, and GPT2 was found to upregulate ADH1A expression in LC cells. Because activation of the mTOR pathway inhibits ADH1A[14], we investigated whether this pathway might mediate GPT2-dependent ADH1A regulation. Using the ARCHS[4] database and experimental validation, we confirmed that GPT2 suppressed mTOR signaling and consequently increased ADH1A expression. This suppression was found to be dependent on GPT2 binding to mTOR, and subsequent disruption of mTOR–AKT interaction and mTOR activation. The effects of GPT2 on mTOR and ADH1A require enzymatic activity. However, this study used only cellular models to assess GPT2 enzymatic function. Future studies should evaluate enzymatically inactive GPT2 mutants or patient-derived samples to further validate the roles of GPT2 activity in LC signaling and gene regulation.

ADH1A is downregulated in several cancers, including non-small cell lung and gastric cancers[10,55], and its loss promotes cancer cell proliferation and migration. Our results were consistent with those from prior reports[14,56]. Diminished ADH1A expression in LC correlated with GPT2 levels. Functionally, ADH1A was found to mediate GPT2-induced suppression of LC cell growth and migration. Given the importance of aberrant lipid metabolism in LC progression, we demonstrated that ADH1A inhibits lipid accumulation. Specifically, ADH1A interacts with LSD1[57], a histone demethylase that promotes lipid synthesis *via* FASN and SCD1 and contributes to LC progression[20,45]. Although we observed a negative correlation between ADH1A and LSD1 in TCGA data (**Figure 4L**), the weak Pearson *r* values indicated the need for validation in larger clinical cohorts. Mechanistically, ADH1A decreases LSD1 expression, thereby downregulating FASN and SCD1 levels and limiting lipid accumulation. Moreover, GPT2-dependent inhibition of lipid accumulation primarily requires ADH1A.

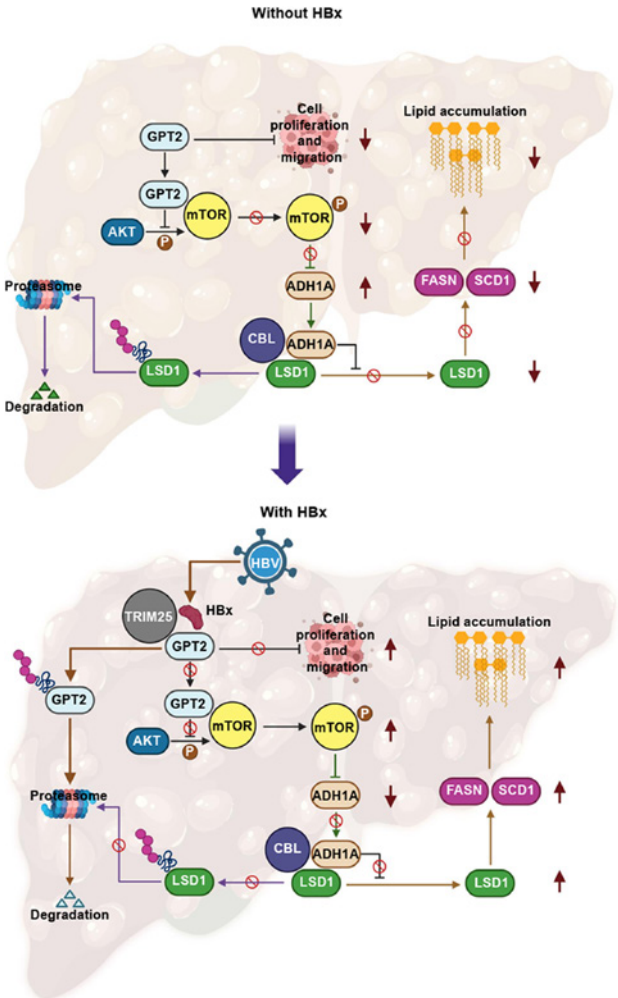


Figure 8 Pattern diagram of the molecular mechanisms through which inhibition of GPT2 expression mediated by HBx restricts ADH1A levels and leads to LC progression, by increasing lipid accumulation, cell proliferation, and migration. Top: In LC cells, GPT2 inhibits LC cell proliferation and migration. Moreover, GPT2 interacts with mTOR, thus attenuating its activation by decreasing the interaction between AKT and mTOR, inhibiting mTOR phosphorylation induced by AKT, and leading to ADH1A upregulation. Subsequently, ADH1A decreases the stabilization of LSD1 *via* interacting with the E3 ubiquitin ligase CBL and promotes binding of CBL to LSD1, thereby facilitating CBL-mediated LSD1 ubiquitination, downregulation of FASN and SCD1 expression, and suppression of lipid accumulation. Bottom: HBx, a viral protein encoded by HBV, inhibits GPT2 expression and consequently restricts ADH1A and enhances LC progression by upregulating LSD1, promoting lipid accumulation, and facilitating cell proliferation and migration. Mechanistically, HBx interacts with GPT2 and suppresses GPT2 stabilization by increasing interaction between the E3 ubiquitin TRIM25 and GPT2, thus promoting GPT2 degradation in a ubiquitin–proteasome-dependent manner. ADH1A, alcohol dehydrogenase 1A; AKT, protein kinase B; CBL, casitas B lineage lymphoma; FASN, fatty acid synthase; GPT2, glutamic-pyruvic transaminase 2; HBx, hepatitis B virus X protein; LC, liver cancer; LSD1, lysine-specific demethylase 1; mTOR, mammalian target of rapamycin; SCD1, stearoyl-CoA decarboxylase 1; TRIM25, tripartite motif containing 25 (created with BioRender. https://app.biorender.com).

We further investigated how ADH1A downregulates LSD1. CBL, an E3 ubiquitin ligase targeting transcription factors such as HIF-1α and p53[58], promotes LSD1 degradation *via* the ubiquitin–proteasome pathway[59]. ADH1A was found to promote CBL-dependent LSD1 destabilization. Moreover, GPT2 inhibited lipid storage in LC cells in an ADH1A-dependent manner. On the basis of the ARCHS[4] database, we predicted that GPT2 and ADH1A positively correlated with fatty acid metabolism and degradation but negatively correlated with NAFLD (**Figure 2**). The functional relevance and mechanisms underlying these predicted associations warrant further investigation.

HBV infection is a major risk factor for hepatocarcinogenesis[23]. HBV decreases GPT2 protein expression in tumor

cells. Among HBV-encoded proteins, HBx is critical for viral replication and carcinogenesis[25,60], as well as modulation of transcription, the cell cycle, autophagy, signaling, apoptosis, and protein degradation[61]. This study demonstrated that HBx mediates HBV-induced GPT2 downregulation. Given the reported role of HBx in promoting lipid storage in LC cells[62,63] we examined the potential involvement of GPT2 inhibition. As expected, HBx silencing of GPT2 suppressed ADH1A expression; increased LSD1, FASN, and SCD1 levels; and enhanced lipid accumulation. HBx was found to promote LC cell proliferation and migration *via* GPT2 downregulation. Because lipid accumulation influences multiple LC cell behaviors[64], GPT2 deficiency is likely to contribute to HBx-driven oncogenic phenotypes. Importantly, HBx promotes TRIM25-mediated ubiquitination and degradation of GPT2. In addition, HBx supports hepatocarcinogenesis through TRIM25-GRP78-MAN1B1 signaling and LASP1/SYVN1-mediated GLUD1 degradation[27,28]. The relative importance of these pathways in HBx-driven LC remains unclear; therefore, their potential as therapeutic targets for HBV-associated LC requires further evaluation.

Conclusions

In summary, GPT2 was found to be downregulated in LC, and its loss suppressed ADH1A, thus increasing LSD1 and lipid accumulation. In HBV-positive LC, HBx was found to inhibit GPT2 expression, in a manner facilitated by TRIM25. These findings provide new insights into HBx-associated hepatocarcinogenesis *via* the TRIM25–GPT2–ADH1A–LSD1 signaling axis. GPT2 overexpression might be a potential treatment strategy for LC, particularly in HBV-driven cases. Factors other than HBV might also contribute to GPT2 downregulation in tumors (**Figure 6D**). Future studies should clarify the mechanism underlying diminished GPT2 expression in HBV-negative LC.

Grant support

This study was supported by the Qing Lan Project of Jiangsu Province, the National Natural Science Foundation of China (Grant No. 82372245), and a Starting Grant for Talents of Xuzhou Medical University (Grant No. RC20552309).

Conflict of interest statement

No potential conflicts of interest are disclosed.

Author contributions

Conceived and designed the analysis: Hongjuan You, Kuiyang Zheng, Chen Li, Renxian Tang, Fanyun Kong.
Collected the data: Xing Wang, Yuxin Wang, Huanyang Zhang, Lihong Ma, Ensi Bao, Yujie Zhong.
Contributed data or analysis tools: Hongjuan You, Xing Wang, Ruyu Liu, Xiucheng Pan.
Performed the analysis: Xing Wang, Xiaocui Li, Suping Qin, Xiangye Liu, Delong Kong.
Wrote the paper: Hongjuan You, Chen Li, Renxian Tang, Fanyun Kong.

Data availability statement

The data generated in this study are available upon request from the corresponding authors.

References

1. Berkemeyer S. Primary liver cancers: connecting the dots of cellular studies and epidemiology with metabolomics. Int J Mol Sci. 2023; 24: 2409.
2. De Martino M, Rathmell JC, Galluzzi L, Vanpouille-Box C. Cancer cell metabolism and antitumour immunity. Nat Rev Immunol. 2024; 24: 654-69.
3. Altea-Manzano P, Decker-Farrell A, Janowitz T, Erez A. Metabolic interplays between the tumour and the host shape the tumour macroenvironment. Nat Rev Cancer. 2025; 25: 274-92.
4. Cao LQ, Xie Y, Fleishman JS, Liu X, Chen ZS. Hepatocellular carcinoma and lipid metabolism: novel targets and therapeutic strategies. Cancer Lett. 2024; 597: 217061.
5. Zhang B, Chen Y, Bao L, Luo W. GPT2 is induced by hypoxia-inducible factor (HIF)-2 and promotes glioblastoma growth. Cells. 2022; 11: 2597.
6. Wu J, Miao C, Wang Y, Wang S, Wang Z, Liu Y, et al. SPTBN1 abrogates renal clear cell carcinoma progression *via* glycolysis reprogramming in a GPT2-dependent manner. J Transl Med. 2022; 20: 603.
7. Mitra D, Vega-Rubin-de-Celis S, Royla N, Bernhardt S, Wilhelm H, Tarade N, et al. Abrogating GPT2 in triple-negative breast cancer inhibits tumor growth and promotes autophagy. Int J Cancer. 2021; 148: 1993-2009.
8. Zhao H, Wu W, Li X, Chen W. Long noncoding RNA UCA1 promotes glutamine-driven anaplerosis of bladder cancer by interacting with hnRNP I/L to upregulate GPT2 expression. Transl Oncol. 2022; 17: 101340.
9. Chi YC, Lee SL, Lai CL, Lee YP, Lee SP, Chiang CP, et al. Ethanol oxidation and the inhibition by drugs in human liver, stomach and small intestine: quantitative assessment with numerical organ modeling of alcohol dehydrogenase isozymes. Chem Biol Interact. 2016; 258: 134-41.
10. Mao G, Mu Z, Wu D. Exosome-derived miR-2682-5p suppresses cell viability and migration by HDAC1-silence-mediated upregulation of ADH1A in non-small cell lung cancer. Hum Exp Toxicol. 2021; 40: S318-30.

11. Guo E, Wei H, Liao X, Xu Y, Li S, Zeng X. Prognostic value of alcohol dehydrogenase mRNA expression in gastric cancer. Oncol Lett. 2018; 15: 5505-16.
12. Gao Q, Zhu H, Dong L, Shi W, Chen R, Song Z, et al. Integrated proteogenomic characterization of HBV-related hepatocellular carcinoma. Cell. 2019; 179: 561-77.e22.
13. Liu X, Li T, Kong D, You H, Kong F, Tang R. Prognostic implications of alcohol dehydrogenases in hepatocellular carcinoma. BMC Cancer. 2020; 20: 1204.
14. Zahid KR, Yao S, Khan ARR, Raza U, Gou D. mTOR/HDAC1 crosstalk mediated suppression of ADH1A and ALDH2 links alcohol metabolism to hepatocellular carcinoma onset and progression *in silico*. Front Oncol. 2019; 9: 1000.
15. Zhang X, Wang X, Wu T, Yin W, Yan J, Sun Y, et al. Therapeutic potential of targeting LSD1/ KDM1A in cancers. Pharmacol Res. 2022; 175: 105958.
16. Yang GJ, Liu YJ, Ding LJ, Tao F, Zhu MH, Shi ZY, et al. A state-of-the-art review on LSD1 and its inhibitors in breast cancer: molecular mechanisms and therapeutic significance. Front Pharmacol. 2022; 13: 989575.
17. Zhang J, Fan X, Zhou Y, Chen L, Rao H. The PRMT5-LSD1 axis confers Slug dual transcriptional activities and promotes breast cancer progression. J Exp Clin Cancer Res. 2022; 41: 191.
18. Shen DD, Pang JR, Bi YP, Zhao LF, Li YR, Zhao LJ, et al. LSD1 deletion decreases exosomal PD-L1 and restores T-cell response in gastric cancer. Mol Cancer. 2022; 21: 75.
19. Malagraba G, Yarmohammadi M, Javed A, Barcelo C, Rubio-Tomas T. The role of LSD1 and LSD2 in cancers of the gastrointestinal system: an update. Biomolecules. 2022; 12: 462.
20. Ma L, Xu A, Kang L, Cong R, Fan Z, Zhu X, et al. LSD1-demethylated LINC01134 confers oxaliplatin resistance through SP1-induced p62 transcription in HCC. Hepatology. 2021; 74: 3213-34.
21. Huang M, Chen C, Geng J, Han D, Wang T, Xie T, et al. Targeting KDM1A attenuates Wnt/β-catenin signaling pathway to eliminate sorafenib-resistant stem-like cells in hepatocellular carcinoma. Cancer Lett. 2017; 398: 12-21.
22. Wu LW, Zhou DM, Zhang ZY, Zhang JK, Zhu HJ, Lin NM, et al. Suppression of LSD1 enhances the cytotoxic and apoptotic effects of regorafenib in hepatocellular carcinoma cells. Biochem Biophys Res Commun. 2019; 512: 852-58.
23. de Martel C, Maucort-Boulch D, Plummer M, Franceschi S. World-wide relative contribution of hepatitis B and C viruses in hepatocellular carcinoma. Hepatology. 2015; 62: 1190-200.
24. Danpanichkul P, Duangsonk K, Chen VL, Saokhieo P, Dejvajara D, Sukphutanan B, et al. Global burden of HBV-related liver disease: primary liver cancer due to chronic HBV infection increased in over one-third of countries globally from 2000 to 2021. Hepatology. 2025; 82: 1274-86.
25. Liu S, Koh SS, Lee CG. Hepatitis B virus X protein and hepatocarcinogenesis. Int J Mol Sci. 2016; 17: 940.
26. Rizzo GEM, Cabibbo G, Craxi A. Hepatitis B virus-associated hepatocellular carcinoma. Viruses. 2022; 14: 986.
27. You HJ, Li Q, Ma LH, Wang X, Zhang HY, Wang YX, et al. Inhibition of GLUD1 mediated by LASP1 and SYVN1 contributes to hepatitis B virus X protein-induced hepatocarcinogenesis. J Mol Cell Biol. 2024; 16: mjae014.
28. You H, Zhang N, Yu T, Ma L, Li Q, Wang X, et al. Hepatitis B virus X protein promotes MAN1B1 expression by enhancing stability of GRP78 via TRIM25 to facilitate hepatocarcinogenesis. Br J Cancer. 2023; 128: 992-1004.
29. You H, Yuan D, Li Q, Zhang N, Kong D, Yu T, et al. Hepatitis B virus X protein increases LASP1 SUMOylation to stabilize HER2 and facilitate hepatocarcinogenesis. Int J Biol Macromol. 2023; 226: 996-1009.
30. You H, Yuan D, Bi Y, Zhang N, Li Q, Tu T, et al. Hepatitis B virus X protein promotes vimentin expression via LIM and SH3 domain protein 1 to facilitate epithelial-mesenchymal transition and hepatocarcinogenesis. Cell Commun Signal. 2021; 19: 33.
31. Ouyang Q, Kavanaugh BC, Joesch-Cohen L, Dubois B, Wu Q, Schmidt M, et al. GPT2 mutations in autosomal recessive developmental disability: extending the clinical phenotype and population prevalence estimates. Hum Genet. 2019; 138: 1183-200.
32. Yan C, Zhou QY, Wu J, Xu N, Du Y, Li J, et al. Csi-let-7a-5p delivered by extracellular vesicles from a liver fluke activates M1-like macrophages and exacerbates biliary injuries. Proc Natl Acad Sci U S A. 2021; 118: e2102206118.
33. Kong F, Li N, Tu T, Tao Y, Bi Y, Yuan D, et al. Hepatitis B virus core protein promotes the expression of neuraminidase 1 to facilitate hepatocarcinogenesis. Lab Invest. 2020; 100: 1602-17.
34. Kong F, Tao Y, Yuan D, Zhang N, Li Q, Yu T, et al. Hepatitis B virus core protein mediates the upregulation of C5α receptor 1 via NF-κB pathway to facilitate the growth and migration of hepatoma cells. Cancer Res Treat. 2021; 53: 506-27.
35. Lachmann A, Torre D, Keenan AB, Jagodnik KM, Lee HJ, Wang L, et al. Massive mining of publicly available RNA-seq data from human and mouse. Nat Commun. 2018; 9: 1366.
36. Lian Q, Wang S, Zhang G, Wang D, Luo G, Tang J, et al. HCCDB: a database of hepatocellular carcinoma expression atlas. Genomics Proteomics Bioinformatics. 2018; 16: 269-75.
37. Edwards NJ, Oberti M, Thangudu RR, Cai S, McGarvey PB, Jacob S, et al. The CPTAC data portal: a resource for cancer proteomics research. J Proteome Res. 2015; 14: 2707-13.
38. Zhang QC, Petrey D, Garzon JI, Deng L, Honig B. PrePPI: a structure-informed database of protein–protein interactions. Nucleic Acids Res. 2013; 41: D828-33.
39. Li Y, Xie P, Lu L, Wang J, Diao L, Liu Z, et al. An integrated bioinformatics platform for investigating the human E3 ubiquitin ligase-substrate interaction network. Nat Commun. 2017; 8: 347.
40. Kong F, You H, Zhao J, Liu W, Hu L, Luo W, et al. The enhanced expression of death receptor 5 (DR5) mediated by HBV X protein through NF-kappaB pathway is associated with cell apoptosis induced by (TNF-α related apoptosis inducing ligand) TRAIL in hepatoma cells. Virol J. 2015; 12: 192.
41. Subramanian A, Tamayo P, Mootha VK, Mukherjee S, Ebert BL, Gillette MA, et al. Gene set enrichment analysis: a knowledge-based approach for interpreting genome-wide expression profiles. Proc Natl Acad Sci U S A. 2005; 102: 15545-50.

42. Hu W, Liu D, Li R, Qian H, Qiu W, Ye Q, et al. Comprehensive analysis of TRIM family genes in hepatitis virus B-related hepatoma carcinoma. Front Genet. 2022; 13: 913743.
43. Dibble CC, Cantley LC. Regulation of mTORC1 by PI3K signaling. Trends Cell Biol. 2015; 25: 545-55.
44. Li X, Bi X. Integrated control of fatty acid metabolism in heart failure. Metabolites. 2023; 13: 615.
45. Abdulla A, Zhang Y, Hsu FN, Xiaoli AM, Zhao X, Yang ES, et al. Regulation of lipogenic gene expression by lysine-specific histone demethylase-1 (LSD1). J Biol Chem. 2014; 289: 29937-47.
46. Soini L, Leysen S, Davis J, Ottmann C. Molecular glues to stabilise protein–protein interactions. Curr Opin Chem Biol. 2022; 69: 102169.
47. Zuo T, Chen P, Jing S, Zhang T, Chang L, Xu F, et al. Quantitative proteomics reveals the development of HBV-associated glomerulonephritis triggered by the downregulation of SLC7A7. J Proteome Res. 2020; 19: 1556-64.
48. Kong F, You H, Kong D, Zheng K, Tang R. The interaction of hepatitis B virus with the ubiquitin proteasome system in viral replication and associated pathogenesis. Virol J. 2019; 16: 73.
49. You H, Kong F, Zhou K, Wei X, Hu L, Hu W, et al. HBX protein promotes LASP-1 expression through activation of c-Jun in human hepatoma cells. J Cell Physiol. 2018; 233: 7279-91.
50. Hao Y, Samuels Y, Li Q, Krokowski D, Guan BJ, Wang C, et al. Oncogenic *PIK3CA* mutations reprogram glutamine metabolism in colorectal cancer. Nat Commun. 2016; 7: 11971.
51. Ji L, Zhang Q, Cao Y, Liu L. A prognostic risk model, tumor immune environment modulation, and drug prediction of ferroptosis and amino acid metabolism-related genes in hepatocellular carcinoma. Hum Cell. 2023; 36: 1173-89.
52. Moreira Franco YE, Alves MJ, Uno M, Moretti IF, Trombetta-Lima M, de Siqueira Santos S, et al. Glutaminolysis dynamics during astrocytoma progression correlates with tumor aggressiveness. Cancer Metab. 2021; 9: 18.
53. Feng XC, Liu FC, Chen WY, Du J, Liu H. Lipid metabolism of hepatocellular carcinoma impacts targeted therapy and immunotherapy. World J Gastrointest Oncol. 2023; 15: 617-31.
54. Paul B, Lewinska M, Andersen JB. Lipid alterations in chronic liver disease and liver cancer. JHEP Rep. 2022; 4: 100479.
55. Ma J, Shi Y, Lu Q, Huang D. Inflammation-related gene ADH1A regulates the polarization of macrophage M1 and influences the malignant progression of gastric cancer. J Inflamm Res. 2024; 17: 4647-65.
56. Mestareehi A. Global gene expression profiling and bioinformatics analysis reveal downregulated biomarkers as potential indicators for hepatocellular carcinoma. ACS Omega. 2024; 9: 26075-96.
57. Ferrarese R, Izzo A, Andrieux G, Lagies S, Bartmuss JP, Masilamani AP, et al. ZBTB18 inhibits SREBP-dependent lipid synthesis by halting CTBPs and LSD1 activity in glioblastoma. Life Sci Alliance. 2022; 6: e202201400.
58. Xiong Y, Xu S, Fu B, Tang W, Zaky MY, Tian R, et al. Vitamin C-induced competitive binding of HIF-1α and p53 to ubiquitin E3 ligase CBL contributes to anti-breast cancer progression through p53 deacetylation. Food Chem Toxicol. 2022; 168: 113321.
59. Chang J, Wang L, Zhou X, Yuan J, Xu W. The CBL-LSD1-CXCL8 axis regulates methionine metabolism in glioma. Cytokine. 2022; 151: 155789.
60. Schollmeier A, Glitscher M, Hildt E. Relevance of HBx for hepatitis B virus-associated pathogenesis. Int J Mol Sci. 2023; 24: 4964.
61. Agustiningsih A, Rasyak MR, Turyadi, Jayanti S, Sukowati C. The oncogenic role of hepatitis B virus X gene in hepatocarcinogenesis: recent updates. Explor Target Antitumor Ther. 2024; 5: 120-34.
62. Cui M, Xiao Z, Sun B, Wang Y, Zheng M, Ye L, et al. Involvement of cholesterol in hepatitis B virus X protein-induced abnormal lipid metabolism of hepatoma cells via up-regulating miR-205-targeted ACSL4. Biochem Biophys Res Commun. 2014; 445: 651-5.
63. Liu Z, Wang J, Liu L, Yuan H, Bu Y, Feng J, et al. Chronic ethanol consumption and HBV induce abnormal lipid metabolism through HBx/SWELL1/arachidonic acid signaling and activate Tregs in HBV-Tg mice. Theranostics. 2020; 10: 9249-67.
64. Gu J, Yao M, Yao D, Wang L, Yang X, Yao D. Nonalcoholic lipid accumulation and hepatocyte malignant transformation. J Clin Transl Hepatol. 2016; 4: 123-30.

Cite this article as: You H, Wang X, Liu R, Wang Y, Zhang H, Ma L, et al. HBx-mediated GPT2 suppression promotes liver cancer development by downregulating ADH1A. Cancer Biol Med. 2026; 23: 888-909. doi: 10.20892/j.issn.2095-3941.2025.0236